Role of Intrinsic and Reflexive Dynamics in the Control of Spinal Stability

Kevin M. Moorhouse

Dissertation submitted to the faculty of the
Virginia Polytechnic Institute & State University
in partial fulfillment of the requirements for the degree of

Doctor of Philosophy

In

Engineering Mechanics

Dr. Kevin P. Granata, chair
Dr. John W. Grant
Dr. Scott L. Hendricks
Dr. John J. Lesko
Dr. Michael L. Madigan
Dr. Yuriko Renardy

September 30, 2005

Blacksburg, Virginia

Keywords: Low back; Dynamics; Intrinsic Stiffness; Reflexes;

Role of Intrinsic and Reflexive Dynamics in the Control of Spinal Stability

Kevin M. Moorhouse

Abstract

Spinal stability describes the ability of the neuromuscular system to maintain equilibrium in the presence of kinematic and control variability, and may play an important role in the etiology of low-back disorders (LBDs). The primary mechanism for the neuromuscular control of spinal stability is the recruitment and control of active paraspinal muscle stiffness (i.e., trunk stiffness). The two major components of active muscle stiffness include the immediate stiffness contribution provided by the intrinsic stiffness of actively contracted muscles, and the delayed stiffness contribution provided by the reflex response. The combined behavior of these two components of active muscle stiffness is often referred to as "effective stiffness".

In order to understand the neuromuscular control of spinal stability, stochastic system identification methods were utilized and nonparametric impulse response functions (IRFs) calculated in three separate studies in an effort to:

1) **Quantify the effective dynamics (stiffness, damping, mass) of the trunk**

Nonparametric IRFs were implemented to estimate the dynamics of the trunk during active voluntary trunk extension exertions. IRFs were determined from the movement following pseudo-random stochastic force disturbances applied to the trunk. Results demonstrated a significant increase in effective stiffness and damping with voluntary exertion forces.

2) **Quantify the reflex dynamics of the trunk**

Nonparametric IRFs were computed from the muscle electromyographic (EMG) reflex response following a similar pseudo-random force disturbance protocol. Reflexes were observed with a mean response delay of 67 msec. Reflex gain was estimated from the peak of the IRF and increased significantly with exertion effort.

3) **Separate the intrinsic and reflexive components of the effective dynamics and determine the relative role of each in the control of spinal stability.**

Both intrinsic muscle and reflexive components of activation contribute to the effective trunk stiffness. To evaluate the relative role of these components, a nonlinear parallel-cascade system identification procedure was used to separate the intrinsic and reflexive dynamics. Results revealed that the intrinsic dynamics of the trunk alone can be insufficient to counteract the destabilizing effects of gravity. This illustrates the extreme importance of reflexive feedback in the maintenance of spinal stability and warrants the inclusion of reflexes in any comprehensive trunk model.

TABLE OF CONTENTS

CHAPTER 1 – BACKGROUND / MOTIVATION……... 1

1.1 Low Back Disorders LBD……..... 1
1.2 Spinal Stability……..…….....3
1.2.1 Mechanical Stability……...……..……..……..... 3
1.2.2 Spinal Stability……...……..... 5
1.3 Effective Stiffness and Dynamics…….……..…7
1.3.1 Description……..…….....7
1.3.2 Measurement of Trunk Stiffness…….....…...9
1.4 Quantification of Reflex……...…….……... 12
1.5 Intrinsic Stiffness vs. Reflexive Stiffness……..... 16
1.6 Project Goals……..... 20

CHAPTER 2 – SYSTEM IDENTIFICATION……..... 21

2.1 System Properties……..... 22
2.1.1 Static vs. Dynamic Systems……....22
2.1.2 Linear vs. Nonlinear Systems……23
2.1.3 Time-Invariant vs. Time-Varying Systems……..... 24
2.2 Nonparametric System identification of LTI Systems……..... 25
2.3 Effects of Measurement Noise……..... 29
2.4 Applications of Nonparametric System identification of LTI Systems... 30
2.5 Subsequent Parameterization of Nonparametric Models……31
2.6 Hammerstein Identification of Nonlinear Systems……34

CHAPTER 3 – TRUNK STIFFNESS AND DYNAMICS DURING ACTIVE EXTENSION EXERTIONS…… 37

3.1 Abstract…… 38
3.2 Introduction…….. 39
3.3 Methods…… 42
3.3.1 Subjects……...42
3.3.2 Experimental Protocol…….. 42
3.3.3 Analyses……..... 45
3.3.4 Error Analysis……47
3.3.5 Statistical Analysis…… 49
3.4 Results……50
3.5 Discussion…….. 53
3.6 Acknowledgement……58

CHAPTER 4 – EFFECTS OF STATIC FLEXION-RELAXATION ON PARASPINAL REFLEX BEHAVIOR……...59

4.1 Abstract……..…60
4.2 Introduction…….....61
4.3 Methods……..64
4.3.1 Subjects……... 64
4.3.2 Protocol……..... 64
4.3.3 Analysis……... 66
4.3.4 Statistical Analysis…… 71
4.4 Results…… 73
4.5 Discussion……...77
4.6 Acknowledgement……83

CHAPTER 5 – INTRINSIC VS. REFLEXIVE COMPONENTS OF EFFECTIVE TRUNK STIFFNESS……84

5.1 Abstract……..85
5.2 Introduction…...……86
5.3 Methods…… 89
5.3.1 Subjects……... 89
5.3.2 Apparatus……... 89
5.3.3 Experimental Protocol……...91
5.3.4 Analysis Procedures…….. 93
5.3.5 Parametric Model……..…. 96
5.3.6 Statistical Analysis……..… 97
5.4 Results…… 99
5.5 Discussion……103
5.6 Acknowledgement……...109

CONCLUSIONS……..… 110

REFERENCES……..…. 113

LIST OF FIGURES AND TABLES

Figure 1.1 Free body diagram of an inverted pendulum model of the trunk ……. 4

Figure 1.2 Typical EMG response to a step change in muscle force ..…….....13

Figure 1.3 Feedback control system representation of trunk reflexes ……..…14

Figure 2.1 Block diagram of a "black box" system ……... 22

Figure 2.2 Block diagram of a Hammerstein system ……..……...……34

Figure 3.1 Experimental setup. The servomotor applied a flexion preload to the trunk and then superimposed a binary pseudorandom stochastic force sequence. The resulting displacement was measured. Subjects were securely strapped into a rigid structure to isolate movement to the trunk ... 43

Figure 3.2A-B Applied trunk force (A) and resulting T10 displacement (B) for a male subject with 100 N preload. Both signals have been filtered using a 75 Hz, low-pass, seventh-order Butterworth filter in software (Matlab, Natick, MA). The dotted line represents the predicted displacement determined by convolving the calculated IRF (Impulse Response Function) with the trunk force sequence applied. The accuracy of the IRF is evident from the displacement variance accounted for (VAF = 93.2 %) ……... 44

Figure 3.3A-B Typical IRFs (Impulse Response Functions) relating trunk displacement to the applied trunk force for two different subjects and the superimposed second-order least-mean-squares fits. This clearly illustrates that a linear second-order model can accurately describe the trunk dynamics. The large variance in effective mass, damping, and stiffness between these two subjects and conditions is evident in the contrast between graphs A and B …… 48

Table 3.1 A-B Displacement VAF (A) and second-order fit accuracy (B) for each gender and preload condition. Gender and preload did not have an effect on VAF or fit accuracy as there was no significant statistical difference between the values at any of the conditions ……. 51

Table 3.2A-B-C Measured effective stiffness (A), effective damping (B), and effective mass (C) for each gender and preload condition. There were no main effects for gender or any significant gender-by-preload interactions. Mean values with similar superscripts were not significantly different ($p > 0.05$) ……. 52

Figure 4.1 Experimental setup. Subject connected to servomotor for data collection ……..…….…. 66

Figure 4.2 Force input, erector spinae EMG output and trunk movement in a female subject after the flexion protocol ……..... 67

Figure 4.3 Impulse Response Function (IRF) for the erector spinae muscle in a female subject after the flexion protocol. The peak reflex gain and rise time are labeled ……..... 70

Figure 4.4 Impulse Response Function (IRF) relating input force perturbation to trunk movement in a female subject. Kinematic gain, G_K is labeled …..…71

Table 4.1 Effects of isotonic trunk extension preload. Mean (standard deviation) of peak reflex gain, latency, and kinematic gain. Results show significant main effects for gender, preload and two-way interactions on reflex gain, G_R, and kinematic gain, G_K ……74

Table 4.2 Effects of flexion-relaxation (FR). Mean (standard deviation) of peak reflex gain, latency, and kinematic gain. Interactions between variables of gender, flexion-relaxation effect, and preload are shown. Significances are indicated by superscripts identified in footnotes ……..……..75

Table 4.3 Mean (standard deviation) of baseline rectus abdominus activity and pelvic angle ……...……76

Figure 5.1 Experimental Setup. The servomotor applied a pseudorandom binary sequence (PRBS) of position perturbations to the T10 level of the trunk and the resulting force was measured. Subjects were securely strapped into a rigid structure to isolate movement to the trunk ……. 90

Figure 5.2 Typical experimental record for a subject maintaining an extension exertion level of 35% MVC with minimal co-contraction ……... 92

Figure 5.3 Block diagram showing the parallel cascade structure comprised of the intrinsic and reflexive contributions to overall trunk force …… 94

Figure 5.4A-B-C Intrinsic force response to a pseudorandom binary sequence of small position perturbations for a subject demonstrating a small positive value of P_{INT} (B) and a subject demonstrating a small negative value of P_{INT} (C) …… 100

Table 5.1 Mean values of the proportional intrinsic response (P_{INT}) and reflexive stiffness parameters (G_{REF}, ζ, w_n) for each experimental condition ……101

Figure 5.5 Reflexive stiffness impulse response function, H_{REF}, along with the superimposed second-order least-squares fit for a subject maintaining an extension exertion level of 20% MVC with minimal co-contraction …….. 102

Chapter 1

Background / Motivation

1.1 Low Back Disorders (LBD)

Chronic low back disorders (LBDs) are a major socio-economic problem which impacts worker productivity, health care expense, and individual suffering (Kelsey and White, 1990). LBDs affect 59 % to 80 % of the population sometime in their lives (Kelsey et al., 1984) leading to substantial morbidity, disability, and economic loss (Praemer et al., 1992; Hollbrook et al., 1994). Among people under 45 years of age, LBDs are the leading cause of activity limitation and affect up to 47 % of workers with physically demanding jobs (Andersson, 1981; Rowe, 1971). The costs associated with LBDs are enormous with recent estimates of total costs to society ranging from $25 billion to $100 billion per year (Cats-Baril and Frymoyer, 1991; Pope, 1996).

Traditionally, assessments of LBD risk focus on factors that influence spinal load (NIOSH, 1981) so that injuries are assumed to occur when compressive spinal load exceeds the injury tolerance or material failure load of the ligamentous spine, discs, and/or vertebrae. However, spinal load often fails to explain injury. Despite incidence rates indicating a significant LBD problem in the automotive industry, Punnett et al. (1991) found less than three percent of sampled jobs imposed static compressive forces greater than the NIOSH recommended action limit of 3400 N (NIOSH, 1981).

Another mode of injury that may explain incidences of LBDs is spinal instability. Clinical analyses indicate unstable structural behavior of the spine may contribute to long-term material damage (Panjabi, 1992). Furthermore, it is well known that structural tolerance is far more fragile than material tolerance in the spine (Crisco and Panjabi,

1992), so spinal stability may play an important role in the etiology of LBDs. In fact, up to 80 % of workplace LBDs may be related to slips or unexpected loads that challenge the stability of the spine (Manning and Shannon, 1981). Injury due to instability of the spine can explain why so many injuries still occur even at loads significantly less than the NIOSH action limit of 3400 N.

1.2 Spinal Stability

1.2.1 Mechanical Stability

Before discussing spinal stability, it is first necessary to understand mechanical stability. Mechanical stability is related to the energy state of a system. Most systems naturally move toward minimum energy configurations. If a desired equilibrium configuration coincides with an energy minimum then the system will naturally move toward or return to the equilibrium state following any perturbation, and is considered stable. A simple example of this is a ball resting inside the bottom of a bowl (McGill and Cholewicki, 2001). Perturbations to the ball will cause it to move to a higher elevation in the bowl (increasing potential energy), but it should subsequently return to the bottom of the bowl toward the minimum energy state. Conversely, if the bowl is turned upside down and the ball is rested on top of the bowl, perturbations to the ball are likely to cause the ball to fall off the bowl onto the table where the energy state is lower.

Another example that is more analogous to the spinal column is a tall thin column of toy blocks that is able to stand in equilibrium. Despite the fact that the column is in equilibrium, if this column is disturbed by a large enough perturbation it will collapse because it is not stable. Furthermore, adding external load to the top of the column compromises stability even further. This is analogous to the spinal column that may satisfy equilibrium but may become unstable and suffer buckling deformation and strain under compressive load.

Figure 1.1 shows a single inverted pendulum with a torsional spring that can be used to represent a very simple model of the trunk. The rigid pendulum represents the spine, the pendulum mass represents the head-arm-trunk (HAT) mass, and the torsional

spring represents the elastic character of the trunk muscles. The potential energy, V, of this pendulum system includes contributions from the gravitational mass, m_{hat}, and the strain energy, K, in the spring:

$$V = m_{hat} gL\cos\vartheta + \frac{1}{2}K(\vartheta - \vartheta_o)^2 \qquad (1.1)$$

where L is the center-of-mass distance from the base of the pendulum, g the acceleration due to gravity, K the rotational stiffness of the controlling spring, and θ and θ_o the angle of the pendulum from vertical and the neutral-angle of the spring respectively.

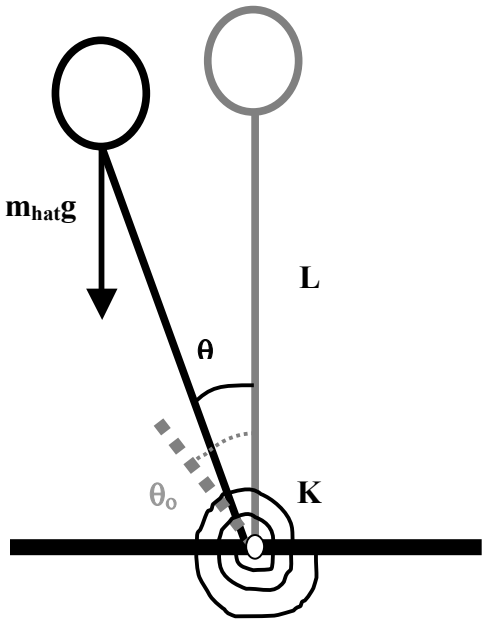

Figure 1.1 Free body diagram of an inverted pendulum model of the trunk

Recall that mechanical stability is related to a minimum energy state and that the mathematical minimum of any single-valued function is identified where the first-derivative is zero (extremum) and the second-derivative is greater than zero (minimum).

In this example the first derivative with respect to pendulum angle is zero in two configurations, standing straight up (θ = 0) or hanging straight down (θ = 180):

$$\frac{\delta V}{\delta \vartheta} = m_{hat} gL \sin \vartheta + K\left(\vartheta - \vartheta_o\right) = 0 \tag{1.2}$$

This indicates that the pendulum can be in equilibrium in either of these two positions, but that does not ensure stability. Stability is achieved when the second-derivative with respect to pendulum angle is greater than zero:

$$\frac{\delta^2 V}{\delta \vartheta^2} = -m_{hat} gL \cos \vartheta + K > 0 \tag{1.3}$$

Equation (1.3) shows that, without stiffness (K = 0), the pendulum can only be stable hanging straight down (θ = 180). In the upright posture, θ = 0, the system is stable for any $K > m_{hat}gL$. This simple model illustrates that sufficient intrinsic stiffness from passive spinal tissues and muscle elastic behavior must be maintained to achieve spinal stability in the absence of feedback.

1.2.2 Spinal Stability

Spinal stability describes the ability of the neuromuscular system to maintain equilibrium in the presence of kinematic and control variability. If the spine is insufficiently stable during loading then there is increased risk that natural kinematic variability (i.e., small kinematic perturbations) or recruitment variability (i.e., small neuromuscular errors) will be amplified by biomechanical forces to cause sudden undesired vertebral motion (localized spinal column buckling) and strain damage of intervertebral tissues (Crisco and Panjabi, 1992; Solomonow et al., 1999). This damage

to the intervertebral tissues can result in intervertebral hyper mobility and potential neuromotor abnormalities. Furthermore, this damage may induce pain, further reduce spinal stability, and enhance the risk of injury or re-injury (Panjabi, 1992).

Factors that contribute to spinal stability at a specific posture and load include stiffness of passive joint tissues, intrinsic stiffness of active muscles (Bergmark, 1989) and associated stiffness from muscle co-recruitment, (Gardner-Morse et al 1995; McGill 2001) as well as proprioception and reflex dynamics (Solomonow et al., 1998). Passive tissues of the ligamentous spine cannot stabilize typical loads without active muscle support (Crisco and Panjabi, 1992). In fact, the ligamentous spine has been found to become unstable, buckle, and fail at compressive loads of 88 N, while typical spinal compression loads within the working environment can exceed 2600 N (Nachemson, 1966). Therefore, intrinsic stiffness of active muscles and reflex response are considered the primary mechanisms for neuromuscular control of spinal stability. To understand neuromuscular control of spinal stability it is necessary to accurately quantify the stiffness and dynamics of the trunk, as well as the reflex response of the stabilizing trunk muscles.

1.3 Effective Stiffness and Dynamics

1.3.1 Description

Stiffness of the trunk may be defined as the dynamic relation between a small perturbation force and the subsequent disturbance to the trunk posture. Musculoskeletal joint dynamics are generally non-linear, as they have been found to vary with level of muscle contraction, perturbation amplitude, and joint angle. However, for small displacements about a prescribed operating point the dynamic behavior is adequately represented by a linear second-order model (Kearney and Hunter, 1990). In other words, for small force or angular perturbations about an approximately constant trunk moment and posture the system dynamics can be represented as a linear second-order system

$$F(t) = M\ddot{\theta} + B(\lambda)\dot{\theta} + K(\lambda)\theta \qquad (1.4)$$

where F(t) is the applied perturbation force, M, B, and K the system mass, damping and stiffness, and θ, $\dot{\theta}$ and $\ddot{\theta}$ represent the perturbation angle, velocity and acceleration. The operating point of the joint is represented by λ and is determined by the level of muscle contraction, perturbation amplitude, and joint angle.

Linear second-order models (equation 1.4) have been utilized extensively in the literature to study joint dynamics. Hunter and Kearney (1982) applied stochastic angular perturbations to the ankle at various levels of baseline muscle contraction and calculated system dynamics (equation 1.4) and stiffness. Likewise, Zhang and Rymer (1997) applied random angular perturbations to the elbow joint and found that elbow joint stiffness increased with baseline muscle contraction. Both of these studies and many like it (Agarwal and Gottlieb, 1977; Granata et al., 2002) obtained accurate results using a

linear second-order model, and found that stiffness and damping increase with baseline muscle contraction.

The stiffness term described in equation (1.4) has both passive and active components. The passive components consist of the intrinsic stiffness of the ligamentous spine as well as the intrinsic stiffness of relaxed trunk muscles. The active components arise from active contraction of the trunk musculature. As described above, it is well documented that joint stiffness increases with baseline muscle contraction (Hunter and Kearney, 1982; Agarwal and Gottlieb, 1977; Zhang and Rymer, 1997; Granata at el., 2002). This difference in mechanics between active and passive muscles can be attributed to the mechanics of a single muscle fiber. Each actively recruited muscle fiber demonstrates elastic stiffness properties, while inactive fibers are comparatively compliant. Muscle fibers are organized in parallel so as increasing numbers of muscle fibers are recruited within a muscle, the net active stiffness increases (McMahon, 1984). Consequently, stiffness of whole active muscle increases in proportion to muscle force (Morgan, 1977).

Besides the steady-state intrinsic stiffness of activated muscles, other active components of the stiffness term in equation (1.4) include the modulation of the contraction level with voluntary response, and the modulation due to the paraspinal reflex response (Nichols & Houk, 1976). Since voluntary response is virtually unpredictable (it varies widely from person to person), most investigators design their experimental protocol to minimize or eliminate its effects. Paraspinal reflexes contribute to the overall dynamics by responding to perturbation movements and associated muscle strain with proportional muscle activation, e.g. feedback (Granata et al., 2004). Unfortunately, time

delay associated with neuromuscular force response diminishes controllability and stability (Stefani et al., 2002). Thus, reflexes do contribute to active muscle dynamics but only after the duration of the reflex delay has been exceeded. Conversely, intrinsic muscle stiffness generates immediate force modulation proportional to the muscle stretch length. Consequently, intrinsic muscle stiffness plays a major role in protecting the lumbar spine from instability events caused by sudden loading/unloading (i.e. slips or falls) (Manning and Shannon, 1981) which may occur too quickly for reflex modulation to occur. The combined behavior of the intrinsic muscle stiffness and the paraspinal reflex response can be referred to as the "effective stiffness" (Cholewicki et al., 2000).

1.3.2 Measurement of Trunk Stiffness

Measurements of trunk stiffness have been reported using diverse experimental methods. The passive stiffness of the trunk has been estimated in anesthetized subjects (Scholten and Veldhuizen, 1986), and in subjects trained to fully relax their trunk musculature (McGill et al., 1994). Considering that the major contributing factor to spinal stability is the recruitment and neuromuscular control of active muscle stiffness, research is necessary to investigate the stiffness of the trunk during active exertions.

Active trunk stiffness has previously been investigated by applying transient step force inputs to the trunk and fitting a second-order model to the resulting kinematic data (Cholewicki et al., 2000; Bull Andersen et al., 2004). Cholewicki (2000) utilized a sudden resisted-force release input, while Bull Andersen (2004) used a rapidly applied load. However, since there was a large step change in trunk moment, equilibrium was

different before and after the disturbance. This means that effective stiffness is changing over the course of the trial because stiffness would change with the level of the muscle force during the equilibrium shift. Therefore the kinematic response is a result of both the effective stiffness of the trunk and the large change in trunk moment and posture during the equilibrium shift. Thus, it would be very difficult to differentiate between these two effects by examining the trunk kinematics. Alternatively, if trunk moment is held constant, maintaining equilibrium, the kinematic response observed would be a result of only the effective stiffness and damping of the trunk. As stated before, linear second-order estimates of trunk dynamics and stiffness are applicable only for small displacements about a prescribed operating point, i.e. equilibrium must be similar before and after the perturbation.

Using a different approach, Gardner-Morse and Stokes (2001) recorded the kinematic response to a single-period, 4 Hz sinusoidal force perturbation. The effective trunk mass and stiffness were estimated by fitting part of the kinematic response (time associated with the first half period of the input force perturbation) to a second-order differential equation of trunk dynamics. Unfortunately, the short period of time used for estimation proved insufficient to measure trunk damping because a minimum of one full period is required to estimate damping. In addition, since only one input driving frequency was investigated, these results may only be valid within a very small frequency range around 4 Hz.

Although each of these studies found that trunk stiffness increases with baseline muscle contraction, the estimated values of trunk stiffness from each were dramatically different when adjusted for differences in baseline experimental conditions such as

muscle contraction level, etc. Published studies demonstrate that improved measurement of joint dynamics and stiffness are possible by applying high-bandwidth, pseudo-random perturbation sequences about a baseline level of muscle contraction (Kearney and Hunter, 1990). As discussed above, similar experimental techniques have been utilized to study the ankle (Hunter and Kearney, 1982; Agarwal and Gottlieb, 1977) and the elbow (Zhang and Rymer, 1997), but have not been attempted in order to quantify effective trunk stiffness and dynamics. Doing so would allow the usage of robust system identification techniques to estimate effective trunk stiffness in a two-step process (Chapter 2). First, characterize the nonparametric dynamics of the system in the form of a vector or curve describing the relation between the input force perturbations and resulting displacement, $F(t) = h(t) * \vartheta(t)$ (See chapter 2). Since this nonparametric curve will provide insight into the system structure and order, the second step is to apply an appropriate parametric model to the nonparametric data to estimate system dynamics, i.e. mass, damping, stiffness. This approach will also provide a goodness-of-fit measure to estimate the validity of the trunk stiffness values.

Effective stiffness and dynamics consist of both the intrinsic stiffness of the trunk musculature and the stiffness due to reflexes. Therefore it would be beneficial to understand and quantify the reflex contribution to trunk stiffness. This will be done by first quantifying reflex response, then calculating the contribution of that reflex to stiffness.

1.4 Quantification of Reflex

Reflex dynamics are among the physiological mechanisms that contribute to musculoskeletal stability. Experimental data suggest that feedback control by means of reflex response may contribute to spinal stability (Granata et al., 2002; Cholewicki and McGill, 1996). Poor reflex response (reduced reflex gain and slowed latency) observed in low back pain patients may play a role in the loss in spinal stability and subsequent low back pain (Luoto et al., 1996; Radebold et al., 2001).

Reflex pathways connecting spinal ligaments to surrounding muscles have been observed (Kang et al., 2002; Solomonow, 1998). Thus, a perturbation force applied to the trunk causes transient tissue strain and excitation of large mechanoreceptors (Golgi, Pacinin, Ruffini fibers) in the spinal ligaments as well as type Ia and type II afferent muscle spindle sensors to initiate reflexive action of the paraspinal muscles (Simon, 1994).

Reflexes can be measured on the surface of the skin overlying the muscles of interest using surface electromyography (EMG). When a muscle is stimulated by a nerve, the neurotransmitter acetylcholine induces Ca^{2+} release from the sarcoplasmic reticulum which surrounds muscle fibers. This triggers voltage dependent Na^{+} and K^{+} channels to open, which creates a depolarization front, called an action potential, which travels through the length of the muscle fiber. Action potentials in the muscle fibers behave in a similar manner to that of a nerve (Berne and Levy, 1998) and can be approximated as a dipole (Enoka, 1994). As the dipole travels, the electric field generated can be measured using differential electrodes parallel to the length of the fiber. By placing electrodes along the length of the muscle fiber, the waveform caused by the

traveling action potential can be recorded from the muscle of interest. Typical EMG response to a step change in muscle force can be seen in Figure 1.2.

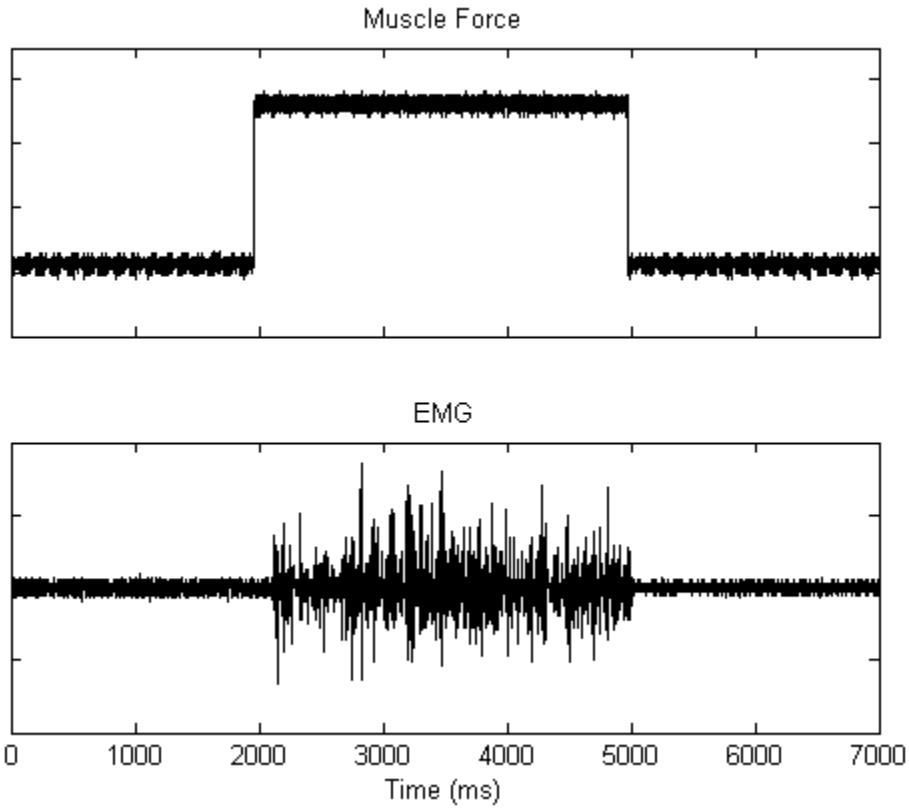

Figure 1.2 Typical EMG response to a step change in muscle force

Paraspinal reflex dynamics can be modeled as a feedback control system (Granata et al., 2004; Matthews, 1991; Solomonow et al., 1998). Shown in Figure 1.3, the open loop path consists of a linear second order differential equation representing the intrinsic dynamics of the trunk (inertia, stiffness, and damping). The output of the open loop path (i.e. angular position of the spine) becomes the input to the feedback segment of the control loop. The feedback segment consists of reflex dynamics and delay. A

perturbation applied to the trunk causes deformation of spinal muscles and ligaments, which directly initiates reflexive action of the paraspinal muscles (Solomonow et al., 1998).

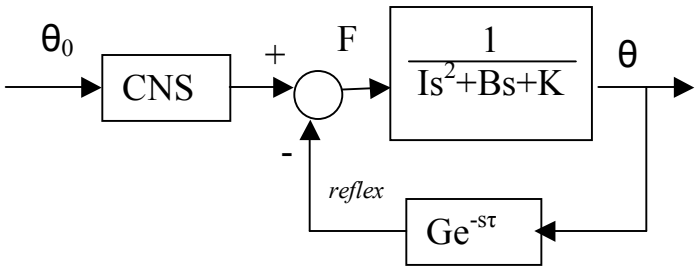

F = Trunk disturbance force
θ = Trunk angular position
G = Feedback (reflex) dynamics
τ = Feedback (reflex) delay
I = Inertia
B = Damping
K = Stiffness
s = Laplace transform

Figure 1.3 Feedback control system representation of trunk reflexes

System identification techniques have previously been employed to quantify reflex dynamics. Zhang et al. (1999) applied patellar tendon taps to elicit a reflex response, and tendon reflex dynamics were estimated using the recorded tapping force as input, and the quadriceps muscle EMG and knee joint extension torque as output. Results indicated that reflex gain increased with background muscle torque.

The stretch reflex dynamics of various muscles about the ankle joint have also been studied (Kearney and Hunter, 1983; Kearney and Hunter, 1984; Kearney and Hunter, 1988). Random angular perturbations were applied to the ankle while baseline muscle contractions of the tibialis anterior (Kearney and Hunter, 1984), triceps surae (Kearney and Hunter, 1983), or gastrocnemius soleus (Kearney and Hunter, 1988) were

maintained. A nonparametric linear impulse response function (Chapter 2) relating velocity of the angular perturbations to EMG of the ankle dorsiflexing muscles (tibialis anterior) was able to accurately describe and quantify the reflex dynamics. However, linear impulse response functions were not able to accurately quantify the reflex dynamics in the ankle plantarflexing muscles (triceps surae or gastrocnemius soleus) even for small perturbations about an operating point. This indicated that a nonlinearity existed in the dynamic relationship relating velocity of angular perturbations to ankle plantarflexing EMG. Therefore, they employed a Hammerstein system identification process (Chapter 2) which was able to identify both the nonlinearity in the system and quantify the reflex dynamics. A direction-dependant nonlinearity (half-wave rectifier) was found, indicating a gross asymmetry between the EMG responses to lengthening and shortening in the ankle plantarflexing muscles. A common result from each of these studies by Kearney and Hunter was that reflex amplitude increased with baseline muscle contraction level but decreased with amplitude of the angular perturbations.

Although paraspinal reflex EMG has been studied elsewhere (Marras et al., 1987; Lavender et al., 1989; Thomas et al., 1998; Krajcarski et al., 1999; Stokes et al., 2000; Wilder et al., 1996; Pope et al., 2000), there have been no published studies to quantify paraspinal reflex dynamics. System identification techniques similar to those applied to the muscles surrounding the ankle joint (see above) could be used to determine and quantify the paraspinal myoelectric response attributable to a force perturbation.

1.5 Intrinsic Stiffness vs. Reflexive Stiffness

As discussed above, effective joint stiffness and dynamics consist of both an intrinsic (non-reflex) component arising from the mechanical properties of the joint, passive tissue, and active muscle fibers, and a reflex component arising from changes in muscle activation due to sensory responses to stretch. The majority of studies regarding joint dynamics (Chapter 1.3) have lumped together the coexisting nonreflex and reflex components. Separation of the intrinsic properties of the joint or muscle in question from the mechanical consequences of reflex is difficult in practice because intrinsic dynamics and reflex dynamics tend to appear and change together.

Initial attempts to isolate the reflex contribution to joint dynamics involved comparing the mechanical contributions of the joint muscles before and after eliminating afferent reflex pathways. This has been accomplished through surgical deafferentation (Nichols and Houk, 1976; Hoffer and Andreassen, 1981), nerve blocks (Herman et al., 1974; Noth et al., 1984; Hufschmidt and Mauritz, 1985), and electrical stimulation of a muscle nerve to override the reflex effects (Houk et al., 1970; Sinkjaer et al., 1988; Carter et al, 1990). These techniques are limited, however, because it is difficult to match the operating points between the reflex-active and reflex-suppressed states exactly. In addition, these approaches are not practical in intact human subjects.

System identification methods have also been utilized to separate the intrinsic and reflex contributions analytically (Kearney et al., 1997; Zhang and Rymer, 1997; Mirbagheri et al., 2000). These analysis techniques utilize the inherent delay in the reflex response in order to separate the intrinsic and reflex effects. Zhang and Rymer (1997) applied random angular perturbations to the ankle while the subject maintained various

levels of baseline muscle contraction and utilized nonlinear delay differential equations to simultaneously solve for the relative contributions of intrinsic mechanical and reflex actions to net joint torque. They found that reflexively-mediated stiffness generated a significant portion of the total joint stiffness, and the percentage varied systematically with baseline muscle contraction level.

Kearney et al (1997) applied a pseudorandom binary sequence of angular perturbations to the ankle and used a nonlinear parallel-cascade system identification technique to separate overall stiffness into intrinsic and reflexive components. Intrinsic stiffness was described by a linear second-order system similar to that in Hunter and Kearney (1982). Reflex dynamics and reflex stiffness were determined using a nonlinear Hammerstein procedure (Chapter 2) and reflex stiffness was described by a standard second-order lowpass system in series with a delay. Since high frequency, vibratory inputs have been shown to inhibit stretch reflexes (Matthews, 1972), velocity and bandwidth of the angular perturbation sequence was varied in order to determine its effect on reflexive stiffness. Reflexive stiffness gain was found to decrease as the mean velocity of the perturbation increased, and intrinsic stiffness was invariant to this change in velocity. Reflex mechanisms were found to be most important at frequencies of 5-10 Hz. This was attributed to the fact that perturbation frequencies less than 5 Hz do not fully activate the muscle spindles (velocity-dependant spindles do not fire), and perturbation frequencies greater than 10 Hz resulted in a large reflex activation but low muscle torque because of the sluggish response of the muscle. In other words, as the frequency increases beyond 10 Hz the reflex activation (EMG) will continue to increase,

but the force of the muscle will not increase because of the lowpass filter nature of muscle mechanics.

In another study by the same group, Mirbagheri et al (2000) used angular perturbations with a velocity which was found optimum to elicit full reflex response (Kearney et al., 1997), in order to determine the variation of intrinsic and reflexive dynamics with activation level and position. The same nonlinear parallel-cascade system identification technique was used, with the exception of a third-order model being necessary to describe reflex stiffness dynamics at high levels of contraction. It was determined that intrinsic stiffness increased monotonically with contraction level, but reflex stiffness was maximal at low contraction levels and then decreased. They also observed various joint angle related differences between intrinsic and reflexive stiffness.

No studies to date have investigated the relative contribution of intrinsic stiffness and reflexive stiffness in the human trunk, so the relative importance of intrinsic dynamics versus reflexes in spinal stability is unknown. Although knowledge of the effective trunk stiffness and dynamics can help determine the likelihood of spinal instability events, we would be better served to understand the role that the two individual components (intrinsic dynamics versus reflexes) play in the maintenance of spinal stability. Since these two components act independently of one another, it is possible that reflexes may be functionally important in some tasks and not in others. In addition, spinal instability events and/or motor control pathology could be caused by malfunction of only the intrinsic dynamics, only the reflex dynamics, or a weighted combination of both. Utilization of parallel-cascade nonlinear system identification

techniques similar to those that have been applied to the ankle can allow for the separation of these effects.

1.6 Project Goals

1) **Quantify the effective dynamics (stiffness, damping, mass) of the trunk (Chapter 3).**

   Trunk stiffness and dynamics during active extension exertions
   Kevin M. Moorhouse, Kevin P. Granata
   Journal of Biomechanics 38 (2005) 2000-2007

2) **Quantify the reflex dynamics of the trunk (Chapter 4).**

   Effects of Static flexion-relaxation on paraspinal reflex behavior
   Kevin P. Granata, Ellen Rogers, Kevin Moorhouse
   Clinical Biomechanics 20 (2005) 16-24

3) **Separate the intrinsic and reflex contributions of the effective dynamics and determine the relative role of each in the control of spinal stability (Chapter 5)**

   Role of Intrinsic and Reflexive Dynamics in the Control of Spinal Stability
   Kevin M. Moorhouse, Kevin P. Granata
   To be published

Chapter 2

System identification

System identification is a process used to build mathematical models of dynamic systems based on measured data from the system (Ljung, 1999). Often the goal is to construct a model that can provide insight into the control behavior of the system. Models obtained from system identification can be classified into parametric models and nonparametric models. Parametric models represent the system in the form of an equation and can produce accurate descriptions of system behavior. However, they require *a priori* knowledge about system structure and order. Nonparametric models are somewhat less efficient computationally, but are ideal for the investigation of unknown systems because their accuracy is not dependant upon *a priori* information. Nonparametric models reveal the true dynamics of the system in the form of a vector or curve, and often the system structure and order can be recognized from this curve and subsequently parameterized. The curve obtained from a nonparametric analysis represents the transfer function or impulse response function (IRF) of the system. The advantage of a nonparametric model is that seemingly random input and output data can be collected with no knowledge of the underlying dynamics, and an IRF can be calculated that represents the true output dynamics subjected to an impulse of the input. This can be advantageous when dealing with previously unknown biomechanical systems.

2.1 System Properties

Systems are often represented as a block diagram (Figure 2.1) in which the "black box", **F,** transforms the input signal, x(t), into the output, y(t). The mathematical description of the transformation is represented by the operator **F**.

Figure 2.1: Block diagram of a "black box" system

This system can be represented in equation form as

$$y(t) = \mathbf{F}\,[x(t)] \tag{2.1}$$

which indicates that when the input x(t) is applied to the system **F**, the output y(t) results. Systems may be characterized by various properties (Oppenheim and Willsky, 1997) which are illustrated in 2.1.1 – 2.1.3.

2.1.1 Static vs. Dynamic Systems

In a static system the current value of the output depends only on the current value of the input so it is considered memoryless. For example, y(t) = sin[x(t)] depends only on the instantaneous value of its input, x(t). Conversely, in a dynamic system, the output depends on some or all of the history of the input. For example, $y(t) = \sum_{\tau} x(t-\tau)$ is dependant on previous values of the input.

Dynamic systems may also be further classified into causal, noncausal, or anticipative systems. Causal systems have outputs which depend on previous, but not future values of their inputs. Noncausal systems have outputs which depend on both the past and future inputs, and anticipative systems have outputs which depend only on future inputs. Most biomechanical systems are causal systems.

2.1.2 Linear vs. Nonlinear Systems

Scalability: Let *a* be a constant scalar. A system is considered to be scalable if multiplying the input by *a* results in output that is multiplied by the same amount:

$$a\mathrm{y}(\mathrm{t}) = \mathbf{F}\,[a\mathrm{x}(\mathrm{t})] \tag{2.2}$$

Additivity: Consider two pairs of inputs and their corresponding outputs,

$$\mathrm{y}_1(\mathrm{t}) = \mathbf{F}\,[\mathrm{x}_1(\mathrm{t})]$$

$$\mathrm{y}_2(\mathrm{t}) = \mathbf{F}\,[\mathrm{x}_2(\mathrm{t})]$$

If the response to the input $\mathrm{x}_1(\mathrm{t}) + \mathrm{x}_2(\mathrm{t})$ is given by:

$$\mathrm{y}_1(\mathrm{t}) + \mathrm{y}_2(\mathrm{t}) = \mathbf{F}\,[\mathrm{x}_1(\mathrm{t}) + \mathrm{x}_2(\mathrm{t})] \tag{2.3}$$

then the system is additive and obeys the property of superposition.

Linear Systems are defined as being both scalable and additive, whereas nonlinear systems do not obey the scalability and additivity principles. Sometimes a nonlinear system may obey scalability and additivity approximately for certain classes of inputs or experimental conditions. In this case the system is operating within its "linear range".

Chapter 1.3 gives examples of nonlinear systems which can be approximated by linear systems under certain experimental conditions.

2.1.3 Time-Invariant vs. Time-Varying Systems

A system is time-invariant if the relationship between the input and output doesn't depend on absolute time. Thus, if y(t) is the response to the input x(t), then the system is time-invariant if y(t - τ) is the response to the input x(t - τ):

$$\text{If } y(t) = \mathbf{F}\,[x(t)] \text{ then } y(t-\tau) = \mathbf{F}\,[x(t-\tau)] \tag{2.4}$$

A system is linear time-invariant (LTI) if it obeys the properties of scalability (Eq. 2.2), additivity (Eq. 2.3), and time-invariance (Eq. 2.4).

2.2 Nonparametric System identification of LTI Systems

Nonparametric system identification is a very powerful analysis technique for linear time-invariant (LTI) systems. The goal of nonparametric system identification is to measure the input and output to a system and then quantify the "black box" properties of the system in the form of an impulse response function (IRF) or transfer function.

A signal x(t) can be interpreted as a string of Dirac delta functions (Oppenheim and Willsky, 1997) or a string of very short pulses as shown in equation (2.5), where δ_Δ is the pulse height, $\delta_\Delta = 1/\Delta$, and Δ is the pulse width.

$$x(t) = \sum_{k=-\infty}^{\infty} x(k\Delta)\delta_\Delta(t - k\Delta)\Delta \tag{2.5}$$

As $\lim \Delta \to 0$, the above sum can be written as an integral of the signal value multiplied by an impulse function (an infinitely high and short pulse with area of unity) as shown in equation (2.6).

$$x(t) = \int_{t=-\infty}^{\infty} x(\tau)\delta(t-\tau)d\tau\,. \tag{2.6}$$

A linear time-invariant system can be described using its response to an impulse. For each instant in time the input signal, x(t), can be considered an impulse function (Eq. 2.6) which will cause a corresponding response to that impulse. In the next moment in time the input signal impulse function will cause another impulse response. Since the system is scalable and time-invariant, the response to the two different impulse functions will be equivalent, except for being scaled to the amplitude value of the input signal. Since the system is additive, the impulse responses can be summed. The output of the system is then simply the sum of all such impulse responses. This mathematical process

is called convolution (equation 2.7), where the output y(t) can be described by the impulse response function (IRF), h(t), convolved (notated with *) with the input x(t).

$$y(t)=\int_{-\infty}^{\infty} x(\tau)h(t-\tau)d\tau = x(t)*h(t) \tag{2.7}$$

Using this property, the response of a system to an arbitrary input can be determined by convolving it with the system's impulse response. Hence, the impulse response function (IRF) provides a complete model of a system's dynamic response in the time domain.

With some algebraic manipulation, the convolution integral can be expressed in terms of the well-known autocorrelation function (Eq. 2.8) and cross-correlation function (Eq. 2.9) (Oppenheim and Willsky, 1997; Ljung, 1999; Hunter and Kearney, 1983). By representing the convolution integral in terms of correlation functions (Eq. 2.14) rather than the input and output signals (Eq. 2.7), the effect of measurement noise is drastically reduced (See Chapter 2.3). The algebraic manipulation required to achieve this is as follows:

The autocorrelation of signal x(t) is described as:

$$c_{xx}(t) = \int_{-\infty}^{\infty} x(\tau)x(t+\tau)d\tau \tag{2.8}$$

whereas the cross-correlation of signals x(t) and y(t) is:

$$c_{xy}(t) = \int_{-\infty}^{\infty} x(\tau)y(t+\tau)d\tau \tag{2.9}$$

Utilizing the time-invariance property with equation (2.7), the input, x(t), and the output, y(t), can be shifted by *r* as shown in equation (2.10)

$$y(t+r)=\int_{-\infty}^{\infty} x(\tau+r)h(t-\tau)d\tau \tag{2.10}$$

Next, both sides are multiplied by x(*r*):

$$x(r)y(t+r) = x(r)\int_{-\infty}^{\infty} x(\tau+r)h(t-\tau)d\tau \tag{2.11}$$

and integrated over *r:*

$$\int_{-\infty}^{\infty} x(r)y(t+r)dr = \int_{-\infty}^{\infty} x(r)\int_{-\infty}^{\infty} x(\tau+r)h(t-\tau)d\tau dr = \int_{-\infty}^{\infty}\int_{-\infty}^{\infty} h(t-\tau)x(r)x(\tau+r)drd\tau \tag{2.12}$$

Equation (2.12) can now be re-written in the form shown below:

$$\int_{-\infty}^{\infty} x(r)y(t+r)dr = \int_{-\infty}^{\infty} h(t-\tau)(\int_{-\infty}^{\infty} x(r)x(\tau+r)dr)d\tau \tag{2.13}$$

It can be seen that the left-hand side of equation (2.13) is in the form of the cross-correlation function (Eq. 2.9) and the right-hand side is the convolution of the IRF with an integral in the form of the autocorrelation function (Eq. 2.8). Therefore, equation (2.13) can be written as:

$$c_{xy}(t) = \int_{-\infty}^{\infty} h(t-\tau)c_{xx}(\tau)d\tau \tag{2.14}$$

For a real system, this integral will have finite limits so it can be represented as:

$$c_{xy}(t) = \int_{T1}^{T2} h(t-\tau)c_{xx}(\tau)d\tau \tag{2.15}$$

where the IRF may be considered trivial when $\tau < T_1$ and $\tau > T_2$.

This integral can be solved numerically by representing this integral in its discrete form:

$$c_{xy}(k) = \Delta t \sum_{i=M1}^{M2} c_{xx}(i)h(k-i) \tag{2.16}$$

where Δt is the sampling rate, $M_1 = \frac{T_1}{\Delta t}$, and $M_2 = \frac{T_2}{\Delta t}$.

Equation (2.16) can be written in matrix form as:

$$C_{xy} = \Delta t \, C_{xx} \, H \tag{2.17}$$

where C_{xy} is an $M_2 - M_1 + 1$ length vector whose i^{th} element is $c_{xy}(M_1 + i - 1)$, C_{xx} is an $M_2 - M_1 + 1$ square matrix whose i, j^{th} element is $c_{xx}(i - j)$, and H is an $M_2 - M_1 + 1$ length vector whose i^{th} element is $h(M_1 + i - 1)$. Finally, this matrix equation can be solved for H, where H will be a vector representing the IRF, i.e. output of the system that would occur given a single impulse of the system input:

$$H = \frac{1}{\Delta t} C_{xx}^{-1} C_{xy} \tag{2.18}$$

The above procedure illustrates a nonparametric time-domain deconvolution technique that can be used to identify the dynamics, H, of a system given measurements of the system input, x(t), and output, y(t).

An additional advantage of this analysis is that it provides an easy goodness-of-fit measure to determine how well the IRF represents the dynamics of the system. The IRF can be convolved with an input sequence of the system in order to obtain a predicted output signal:

$$y_{pred}(t) = \int x(\tau) H(t - \tau) d\tau \tag{2.19}$$

where $H(t)$ is estimated from measured data (Eq. 2.18). The variance accounted for (VAF %) can then be calculated between the actual and predicted output signals as in equation (2.20):

$$VAF = 100\left(1 - \frac{\sum \left(y_{meas}(t) - y_{pred}(t)\right)^2}{\sum \left(y_{meas}(t)\right)^2}\right) \tag{2.20}$$

VAF equal to 100 % indicates the estimated IRF, $H(t)$, is able to exactly predict the measured output signal from the input signal.

2.3 Effects of Measurement Noise

In real systems it is often unrealistic to assume that noise, n(t), will not be introduced into the measurement of the output signal, y(t). Therefore, the observed signal, z(t), is not always the true output of the system, but more likely:

$$z(t) = y(t) + n(t) \tag{2.21}$$

or

$$z(t) = \int x(\tau)h(t-\tau)d\tau + n(t) \tag{2.22}$$

Using correlation functions, this can be written as

$$c_{xz}(t) = \int h(t-\tau)c_{xx}(\tau)d\tau + c_{xn} \tag{2.23}$$

where c_{xn} is the cross-correlation function between x(t) and n(t). As long as the noise is not correlated with the input, c_{xn} approaches zero so the effects of random noise are very small (Godfrey, 1980). In some cases there may be some process noise or data sampling artifact that is correlated with the input which can result in very noisy IRF estimations. Published techniques illustrate that adding white noise to the input signal will reduce this effect by decorrelating the noise from the input signal (Ljung, 1999).

2.4 Applications of Nonparametric System identification of LTI Systems

Nonparametric system identification can be applied to any dynamic system as long as both the input and the output of the system can be measured. The IRF then represents the dynamic relationship between the input and output. If the input is displacement and the output is force then the IRF represents the dynamic relationship between position and torque, otherwise known as stiffness (impedance) dynamics. Conversely, if the input is force and the output is displacement then the IRF represents the dynamic relationship between force and position, otherwise known as compliance dynamics (Chapter 3). As a final example, if the input is force and the output is EMG then the IRF represents the reflex dynamics (Chapter 4).

2.5 Subsequent Parameterization of Nonparametric Models

In some cases, inspection of the shape of the IRF reveals information about the system's structure and order. For example, the compliance dynamics of the trunk appear very similar to a second-order, underdamped system exhibiting one oscillation (Chapter 3). Therefore, the parameters of the dynamic relationship of the system (i.e., mass, damping, and stiffness) can be obtained by determining the best least-squares fit between the nonparametric IRF and a typical second-order system. Typical second-order systems can be represented in the time-domain as:

$$\hat{H}(t) = Ae^{-Bt}\sin(\omega_d t) \tag{2.24}$$

where A is the undamped amplitude, B is the damping coefficient, and ω_d is the damped natural frequency. The values of A, B, ω_d that best approximate the dynamics of the system can be selected by determining the values of these three parameters that minimize the least-squares error (LSE) between the estimated $\hat{H}(t)$ and the actual IRF, H(t):

$$LSE = \frac{\sum_t \left(H(t) - \hat{H}(t)\right)^2}{\sum_t \left(H(t)\right)^2} \tag{2.25}$$

More useful, however, would be to know the system mass, damping, and stiffness. These values can be obtained from the typical Laplace representation of a second-order system:

$$\hat{H}(s) = \frac{G\omega_n^2}{s^2 + 2\zeta\omega_n s + \omega_n^2} \tag{2.26}$$

where G is the static gain, ζ is the damping parameter, ω_n is the undamped natural frequency, and s is the Laplace variable.

The inverse Laplace transform of equation (2.26) yields the time-domain representation:

$$\hat{H}(t) = \frac{G\omega_n}{\sqrt{1-\zeta^2}} e^{-\zeta\omega_n t} \sin \omega_n \sqrt{1-\zeta^2}\, t \tag{2.27}$$

Comparison of equation (2.27) with equation (2.24) demonstrates the following relationships between the measured parameters A, B, and ω_d with G, ω_n, and ζ:

$$A = \frac{G\omega_n}{\sqrt{1-\zeta^2}} \tag{2.28}$$

$$B = \zeta\omega_n \tag{2.29}$$

$$\omega_d = \omega_n \sqrt{1-\zeta^2} \tag{2.30}$$

After using these relationships to calculate G, ω_n, and ζ, we can determine the system mass, damping, and stiffness by examining the other common Laplace representation of a second-order system:

$$\hat{H}(s) = \frac{1}{ms^2 + bs + k} \tag{2.31}$$

where m, b, and k are the system mass, damping, and stiffness, respectively. Comparison of equation (2.31) with equation (2.26) yields the following relationships to obtain system mass, damping, and stiffness:

$$m = \frac{1}{G\omega_n^2} \tag{2.32}$$

$$b = \frac{2\zeta}{G\omega_n} \tag{2.33}$$

$$k = \frac{1}{G} \tag{2.34}$$

Sometimes the system dynamics are more complicated than a simple second-order system. For example, Kearney (1997) parameterized the reflexive stiffness IRF of the ankle using a second-order model in series with a delay:

$$\hat{H}_{RS} = \frac{G}{s^2 + 2\zeta\omega_n s + \omega_n^2} e^{-sT} \tag{2.35}$$

Mirbagheri (2000) found that for high values of muscle activation, the reflexive stiffness IRF of the ankle was best parameterized using a third-order model in series with a delay:

$$\hat{H}_{RS} = \frac{G\omega_n^2 p}{(s^2 + 2\zeta\omega_n s + \omega_n^2)(s + p)} e^{-sT} \tag{2.36}$$

where p is the first-order cut-off frequency. In these more complicated models a Levenberg Marquardt nonlinear least-square fit algorithm (Press et al., 1985) was employed to find the best "least-squares" fit to the IRF.

2.6 Hammerstein Identification of Nonlinear Systems

The LTI methods illustrated in Chapter 2.2 will produce poor results for nonlinear systems. One method of identifying the dynamics of a nonlinear system is the Hammerstein approach. A Hammerstein system is modeled as a static nonlinear system, n(.), followed by a dynamic linear system, h(τ), as seen in Figure 2.2.

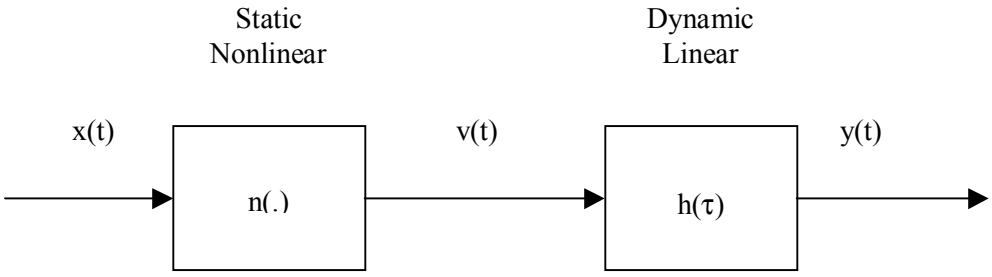

Figure 2.2 Block diagram of a Hammerstein system

x(t) = system input; **n(.) = static nonlinearity in system**

y(t) = system output; **v(t) = output of static nonlinearity**

h(τ) = linear IRF between nonlinearly transformed input and output

An iterative approach to identify both the nature of the static nonlinearity and the system dynamics has been developed by Hunter and Korenberg (1986). Essentially, each iteration attempts to refine two separate estimates of the intermediate signal, $\hat{v}(t)$ and $\hat{v}_{alt}(t)$. The algorithm proceeds as follows:

1) Estimate the inverse linear impulse response function $\hat{h}^{-1}(\tau)$ between the output, y(t) and the input, x(t).

2) Compute the "primary" estimate of the intermediate signal, $\hat{v}(t)$, with the convolution: $\hat{v}(t) = \hat{h}^{-1}(\tau) * y(t)$.

3) Fit a high-order polynomial, $\hat{n}(.)$, between the input x(t) and the current estimate of the intermediate signal, $\hat{v}(t)$.

4) Predict an "alternate" estimate of the intermediate signal, $\hat{v}_{alt}(t) = \hat{n}(x(t))$.

5) Estimate a new linear impulse response function, $\hat{h}(\tau)$, between $\hat{v}_{alt}(t)$ and the output, y(t).

6) Generate the predicted output, $\hat{y}(t) = \hat{h}(\tau) * \hat{v}_{alt}(t)$, and compute the mean-square error (MSE) between the predicted output, $\hat{y}(t)$, and the actual output, y(t). Compare this MSE with the MSE calculated in the previous iteration. If the error does not improve significantly the iteration process is done and the static nonlinearity and the system dynamics are contained in $\hat{n}(.)$ and $\hat{h}(\tau)$, respectively. If the error improves or this is the first iteration, continue.

7) Estimate a new inverse linear impulse response function $\hat{h}^{-1}(\tau)$, between the output, y(t), and $\hat{v}_{alt}(t)$. Return to step 2.

Kearney and Hunter (1983; 1988) have shown that a Hammerstein identification procedure is able to accurately quantify the reflex dynamics and nonlinear nature of the plantarflexing ankle muscles. This process will be used to determine the reflex dynamics and reflexive stiffness of the trunk (Chapter 5).

Chapter 3

Trunk Stiffness and Dynamics during Active Extension Exertions

Kevin M. Moorhouse, M.S.

Kevin P. Granata, Ph.D.

Journal of Biomechanics 38 (2005) 2000-2007

Musculoskeletal Biomechanics Laboratories
Department of Engineering Science & Mechanics
School of Biomedical Engineering and Science
Virginia Polytechnic Institute & State University
219 Norris Hall (0219)
Blacksburg, VA 24061

Address all correspondence to: K.P. Granata, Ph.D.
Musculoskeletal Biomechanics Laboratories
Department of Engineering Science & Mechanics
School of Biomedical Engineering and Science
Virginia Polytechnic Institute & State University
219 Norris Hall (0219)
Blacksburg, VA 24061
Phone: (540) 231-5316
FAX: (540) 231-4547
Granata@VT.edu

Keywords: Low-Back; Dynamics; Stiffness; Model

3.1 Abstract

Spinal stability is related to the recruitment and control of active muscle stiffness. Stochastic system identification techniques were used to calculate the effective stiffness and dynamics of the trunk during active trunk extension exertions. Twenty-one healthy adult subjects (10 males, 11 females) wore a harness with a cable attached to a servomotor such that isotonic flexion preloads of 100 N, 135 N, and 170 N were applied at the T10 level of the trunk. A pseudo-random stochastic force sequence (bandwidth 0-10 Hz, amplitude ± 30 N) was superimposed on the preload causing small amplitude trunk movements. Nonparametric impulse response functions (IRFs) of trunk dynamics were computed and revealed that the system exhibited underdamped second-order behavior. Second-order trunk dynamics were determined by calculating the best least-squares fit to the IRF. Quality of the model was quantified by comparing estimated and observed displacement variance accounted for (VAF), and quality of the second-order fits were calculated as a percentage and referred to as fit accuracy. Mean VAF and fit accuracy were 87.8 ± 4.0% and 96.0 ± 4.3 %, respectively, indicating the model accurately represented active trunk kinematic response. The accuracy of the kinematic representation was not influenced by preload or gender. Mean effective stiffness was 2.78 ± 0.96 N/mm and increased significantly with preload ($p < .001$), but did not vary with gender ($p = .425$). Mean effective damping was 314 ± 72 N-s/m and effective trunk mass was 37.0 ± 9.3 kg. We conclude that stochastic system identification techniques should be used to calculate effective trunk stiffness and dynamics.

3.2 Introduction

Recruitment and control of active muscle stiffness contributes to spinal stability (Bergmark, 1989; Gardner-Morse et al, 1995). Stiffness of the trunk may be defined as the dynamic relation between a small perturbation force and the subsequent trunk displacement. Musculoskeletal joint dynamics are generally non-linear. However, for small force or angular perturbations about a prescribed operating point (approximately constant trunk moment and posture) the system dynamics can be adequately represented by a linear second-order model (Kearney and Hunter, 1990). Small angular or force perturbations about various levels of mean joint torque have been utilized to calculate the joint stiffness and dynamics in the ankle (Hunter and Kearney, 1982; Agarwal and Gottlieb, 1977), elbow (Zhang and Rymer, 1997), and the knee (Granata et al., 2002). Each of these studies obtained accurate results using a linear second-order model and found that stiffness increases with increased active joint torque. Research concludes that the apparent stiffness of a joint contains both intrinsic components and reflexive components (Nichols & Houk, 1976). Paraspinal muscle reflexes contribute to spinal stability by responding to perturbation movements and associated muscle strain with proportional muscle activation (Granata et al., 2004). This proportional reflex response contributes to the overall stiffness of the joint and the combined behavior of the intrinsic muscle stiffness and the reflex response can be referred to as the "effective stiffness" (Cholewicki et al., 2000).

Measurements of trunk stiffness have been reported using diverse experimental methods. The passive stiffness of the trunk has been estimated in anesthetized subjects (Scholten and Veldhuizen, 1986), and in subjects trained to fully relax their trunk

musculature (McGill et al., 1994). Considering that the major contributing factor to spinal stability is the recruitment and neuromuscular control of active muscle stiffness, research is necessary to investigate the stiffness of the trunk during active exertions. Active trunk dynamics have previously been investigated by applying either transient (Cholewicki et al., 2000; Bull Andersen et al., 2004) or sinusoidal (Gardner-Morse and Stokes, 2001) force inputs to the trunk and fitting a second-order model to the resulting kinematic data. Cholewicki (2000) utilized a sudden resisted-force release input, while Bull Andersen (2004) used a rapidly applied load. However, since there was a large step change in trunk moment, equilibrium was different before and after the disturbance making it difficult to differentiate between the effects of the neuromuscular change from one equilibrium condition to another versus that of effective stiffness and damping. Specifically, linear second-order estimates of trunk dynamics and stiffness are applicable only for small displacements about a prescribed operating point, i.e. equilibrium must be similar before and after the perturbation. Gardner-Morse and Stokes (2001) maintained trunk equilibrium by applying single-period, 4 Hz sinusoidal force perturbations, but the short period of time used for estimation proved insufficient to measure trunk damping, thus it was neglected. In addition, since only one input driving frequency was investigated, these results may only be valid within a very small frequency range around 4 Hz. Although each of these studies found that trunk stiffness increases with preload, the estimated values of trunk stiffness from each were dramatically different when adjusted for differences in baseline experimental conditions such as trunk moment preload etc. Published studies demonstrate that improved measurement of joint dynamics

and stiffness are possible with high-bandwidth, pseudo-random perturbation sequences about a baseline bias torque (Kearney and Hunter, 1990).

These methods can be applied to accurately estimate effective trunk stiffness in a two-step process. First, characterize the nonparametric dynamics of the system in the form of a vector or curve describing the relation between the input force perturbations and resulting displacement. Since this nonparametric curve provides insight into the system structure and order, the second step is to apply an appropriate parametric model to the nonparametric data to estimate system dynamics, i.e. mass, damping, stiffness. This approach also provides a goodness-of-fit measure to estimate the validity of the trunk stiffness values.

The goal of this study was to quantify effective trunk stiffness during active trunk extension exertions. It was hypothesized that by using high-bandwidth pseudo-random force perturbation sequences applied to the trunk that 1) the nonparametric impulse response function (IRF) can accurately describe the dynamics of the trunk, 2) a linear second-order model can accurately fit the system dynamics of the trunk, and 3) effective trunk stiffness will increase with steady-state trunk extension preload.

3.3 Methods

3.3.1 Subjects

Twenty-one subjects with no previous history of low back pain participated after signing informed consent approved by the institutional review board at Virginia Tech. Subjects included ten males (mean age 23.5 ± 3.2 years, mean height 183.2 ± 8.4 cm, mean weight 83.4 ± 12.7 kg) and eleven females (mean age 20.4 ± 1.5 years, mean height 164.5 ± 7.2 cm, mean weight 57.7 ± 10.2 kg).

3.3.2 Experimental Protocol

Each subject stood upright in a pelvic restraint structure designed to restrict the motion of the lower body (Fig. 3.1). A harness and cable system attached the subject to a servomotor (Pacific Scientific, Rockford, Ill) such that the cable tension applied flexion loads at the T10 level of the trunk. The motor was programmed to provide three levels of isotonic preload, 100 N, 135 N, and 170 N. These preloads required paraspinal muscle preactivation to maintain upright equilibrium of the trunk. Left and right rectus abdominus EMG was displayed on an oscilloscope in plain sight of the subject, and subjects were instructed to keep this antagonistic muscle activity to a minimum in order to reduce unnecessary co-contraction. Once this was accomplished, force perturbations of ± 30 N were superimposed on the preload in a binary pseudorandom stochastic fashion (Fig. 3.2A) with a flat bandwidth from 0-10 Hz. Pseudorandom stochastic inputs were chosen to avoid problems with voluntary responses due to predictable stimuli as recommended by Kearney and Hunter (1990). The applied forces were measured by a

torque transducer (Omega TQ301 series, 0-45 N-m, Stamford, CT) attached to the shaft of the motor and sampled at 1000 Hz. The small amplitude trunk kinematics in response to the perturbation forces were recorded using two OPTOTRAK infrared emitting diodes (Fig. 3.2B, solid line) (Northern Digital, Waterloo, Ontario, Canada). Sensors were placed using double-sided tape over the subject's spinous processes palpated at S1 and T10, and were recorded at 200 Hz using a 16 channel A/D converter (Northern Digital, Waterloo, Ontario, Canada).

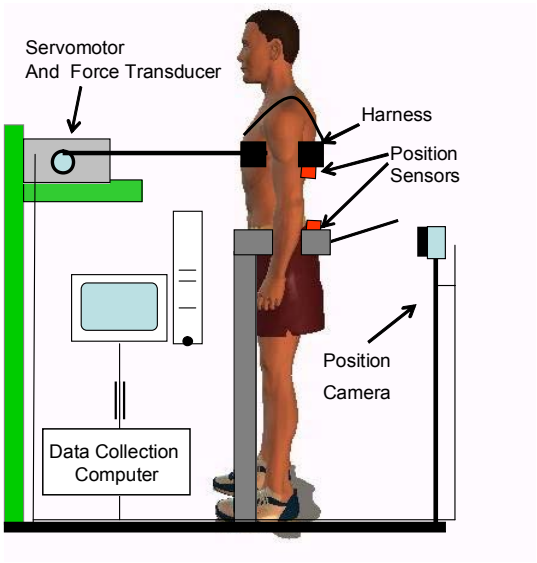

Fig. 3.1. Experimental setup. The servomotor applied a flexion preload to the trunk and then superimposed a binary pseudorandom stochastic force sequence. The resulting displacement was measured. Subjects were securely strapped into a rigid structure to isolate movement to the trunk.

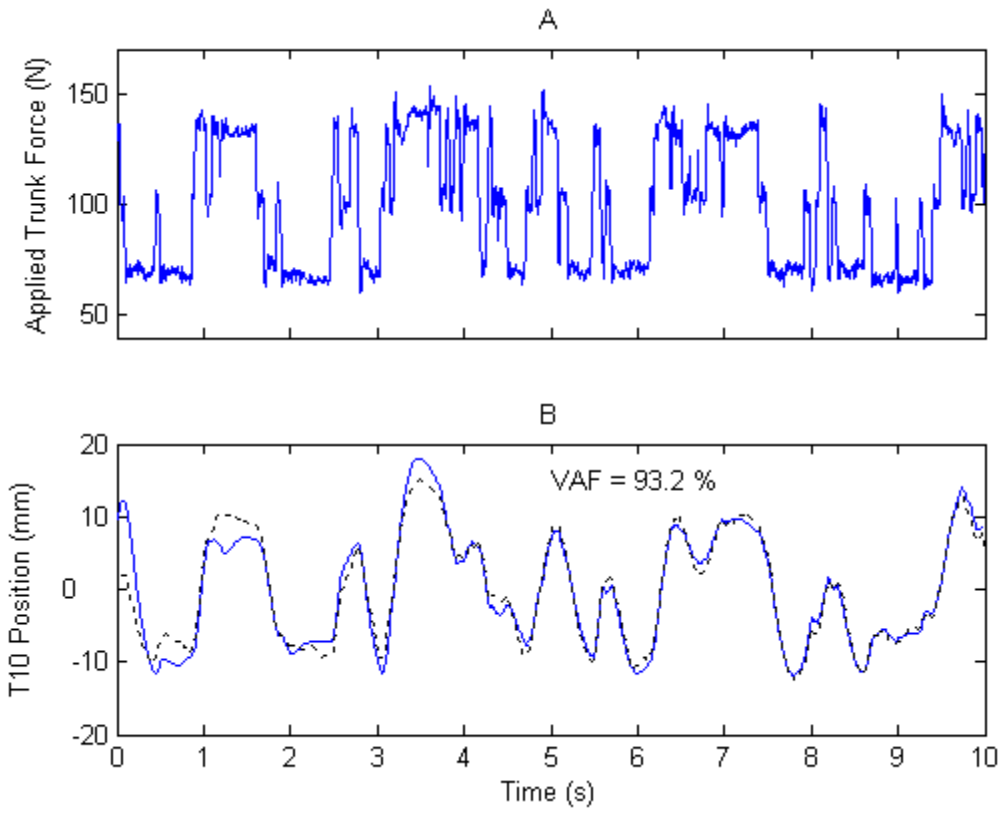

Fig. 3.2A-B. Applied trunk force (A) and resulting T10 displacement (B) for a male subject with 100 N preload. Both signals have been filtered using a 75 Hz, low-pass, seventh-order Butterworth filter in software (Matlab, Natick, MA). The dotted line represents the predicted displacement determined by convolving the calculated IRF (Impulse Response Function) with the trunk force sequence applied. The accuracy of the IRF is evident from the displacement variance accounted for (VAF = 93.2 %).

Three perturbation trials of ten seconds each were performed at each preload level for a total of nine data trials presented in random order. The force and displacement signals were inspected visually to assure data quality. Twenty-one of the 189 trials collected were thrown out due to sections of missing OPTOTRAK data presumably caused by the subject's clothing or hair blocking the infrared emitting diode. Both force and displacement signals were demeaned and filtered using a 75 Hz, low-pass, seventh-

order Butterworth filter using Matlab (The Mathworks, Inc., Natick, MA) to avoid aliasing then sub-sampled at 200 Hz (Bendat and Piersol, 2000). Signal quality was improved by adding white noise with amplitude equal to 30% of one standard deviation of the input trunk force to the input signal in order to decorrelate process noise and data sampling from the input signal (Ljung 1999).

3.3.3 Analyses

To quantify trunk stiffness, the nonparametric compliance IRF relating the pseudorandom force input and the T10 displacement was determined. This IRF was computed from the matrix solution relating the force autocorrelation function and the force/displacement cross-correlation function similar to that discussed in Hunter and Kearney (1983).

Calculation of the nonparametric compliance IRF was based on well known time domain deconvolution techniques, and assumes a linear time-invariant (LTI) system. The output y(t), i.e., trunk displacement, was described by the impulse response function h(t) of the system convolved (notated with *) with the applied input trunk force, x(t):

$$y(t) = \int_{T_1}^{T_2} h(\tau)x(t-\tau)d\tau = h(t) * x(t) \tag{3.1}$$

where $h(\tau)$ may be considered trivial when $\tau < T_1$ and $\tau > T_2$. Equation 3.2 may be represented in discrete time by:

$$y(i) = \Delta t \sum_{j=M_1}^{M_2} h(j)x(i-j) \tag{3.2}$$

where the input, x(i), and the output, y(i), are sampled every Δt seconds, $M_1 = \frac{T_1}{\Delta t}$, and $M_2 = \frac{T_2}{\Delta t}$. Using this property, any LTI system can be described in its entirety by its impulse response function (IRF) because once h(t) is known, the output of the system can be determined for any input. With some algebraic manipulation it is easy to express equation 3.2 in terms of the input autocorrelation function, c_{xx}, and the input/output cross-correlation function, c_{xy}:

$$c_{xy}(k) = \Delta t \sum_{j=M_1}^{M_2} h(j) c_{xx}(k-j) \tag{3.3}$$

This equation can then be written in matrix form and solved for H to obtain:

$$H = \frac{1}{\Delta t} C_{xx}^{-1} C_{xy} \tag{3.4}$$

where C_{xy} is an $M_2 - M_1 + 1$ length vector whose i^{th} element is $c_{xy}(M_1 + i - 1)$, C_{xx} is an $M_2 - M_1 + 1$ square matrix whose i, j^{th} element is $c_{xx}(i - j)$, and H is an $M_2 - M_1 + 1$ length vector whose i^{th} element is $h(M_1 + i - 1)$. H will be a vector representing the IRF, i.e. trunk displacement which would occur given a single force impulse.

Quality of the IRF was quantified by comparing displacements predicted by the IRF, $Displacement_{predicted}$ (Fig. 3.2B, dotted line), with measured displacements, $Displacement_{actual}$ (Fig. 3.2B, solid line), in terms of the percentage of variance accounted for (VAF):

$$VAF = 100\left(1 - \frac{\sum \left(Displacement_{actual} - Displacement_{predicted}\right)^2}{\sum \left(Displacement_{actual}\right)^2}\right) \tag{3.5}$$

Predicted displacement was estimated by convolving the IRF with the measured pseudorandom force sequence. VAF equal to 100% indicates the IRF exactly predicts the measured trunk displacement signal from the input force perturbations.

Inspection of the IRF shapes revealed that the system appeared very similar to a second-order, underdamped system exhibiting one oscillation (Fig. 3.3A-B). Therefore, the nonparametric IRFs were subsequently parameterized by least-squares fit to a second-order system

$$H(s) = \frac{1}{ms^2 + bs + k} \tag{3.6}$$

where m is the effective trunk mass, b is the effective trunk damping, k is the effective trunk stiffness, and s is the Laplace variable. Damping and stiffness are referred to as "effective" because they consist of both intrinsic and reflexive components; mass is referred to as "effective mass" because we are representing the trunk by a single rigid mass and spring. The flexible attachments between vertebrae as well as the effects of the head and arms will cause the effective mass to be somewhat lower than the actual trunk mass. The quality of the second-order fits obtained was calculated as a percentage and referred to as fit accuracy.

3.3.4 Error Analysis

Prior to subject testing, the analysis procedure was validated by using the methods described above to calculate the mass and effective stiffness of a known spring-mass system. In this case the calculated mass would be the actual mass rather than an effective

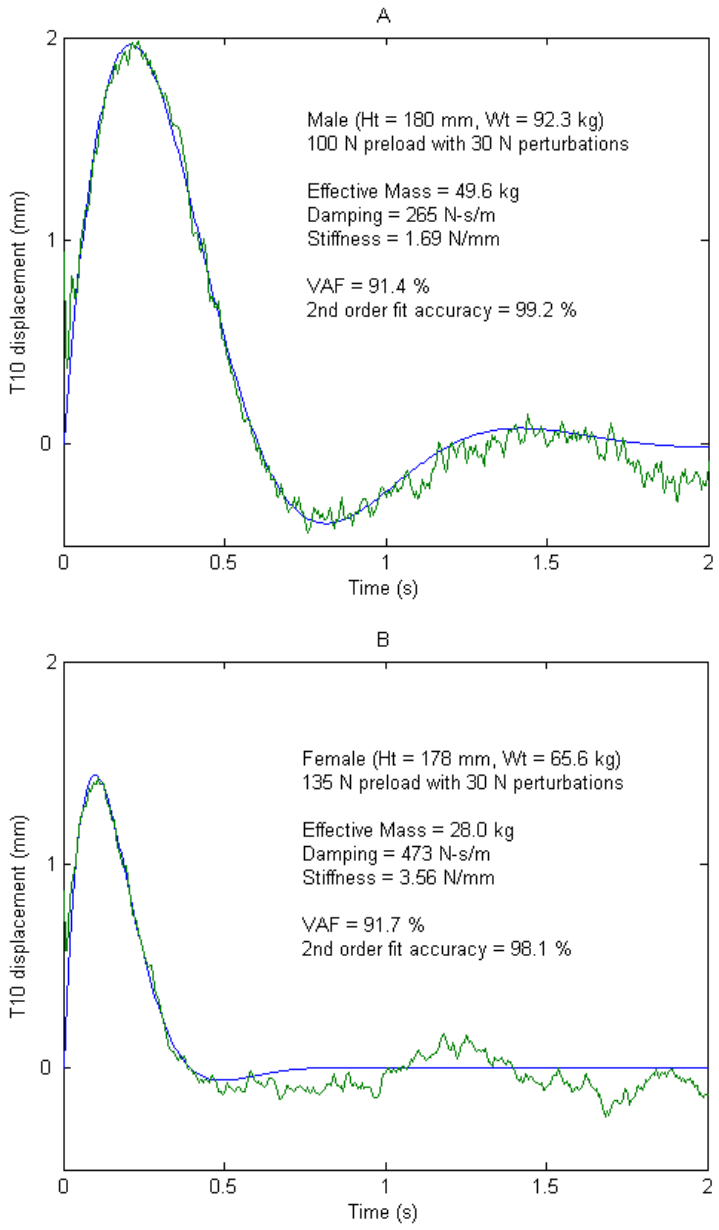

Fig. 3.3A-B. Typical IRFs (Impulse Response Functions) relating trunk displacement to the applied trunk force for two different subjects and the superimposed second-order least-mean-squares fits. This clearly illustrates that a linear second-order model can accurately describe the trunk dynamics. The large variance in effective mass, damping, and stiffness between these two subjects and conditions is evident in the contrast between graphs A and B.

mass because the system is a single rigid mass and spring system. A spring with stiffness similar to that of the trunk (2.38 N/mm) was attached to the servomotor in series with a mass that ranged from 6.82 kg (15 lb) to 34.09 kg (75 lb). These values of mass were chosen in order to provide a wide range of test masses while approaching the average trunk mass at the upper end. Stochastic force perturbations similar to our protocol were applied and the resulting displacement was measured. The nonparametric IRF was calculated and subsequently fit to a second-order model.

3.3.5 Statistical Analysis

Statistical repeated measures analyses (ANOVA) were performed to determine the effect of preload on the second-order parameters, m, b, and k. The independent variable of gender was analyzed as a between subject variable while preload was analyzed as a within subject variable. Analyses were performed using commercial statistical software (Statistica, 5, Statsoft, Inc., Tulsa, OK) using a significance level of $\alpha < 0.05$ for all tests. Trends in significant variables were investigated using Tukey honest significant difference (HSD) post-hoc analyses.

3.4 Results

An error analysis of the methods used to calculate trunk stiffness was performed on a known spring-mass system consisting of a spring with a stiffness of 2.38 N/mm in series with a mass that ranged from 6.82 kg (15 lb) to 34.09 kg (75 lb). The average error between calculated mass and actual mass was 0.87 ± 0.34 kg and the average error between calculated stiffness and actual stiffness was 0.022 ± 0.011 N/mm. Since these results represent only a 0.92% error in stiffness and a 4.3% error in mass, the analysis methods in this study were considered accurate enough to proceed with subject testing.

The compliance IRFs calculated in this study were able to accurately predict the active trunk kinematic response to random applied trunk forces, as evidenced by the high values of displacement variance accounted for (VAF). VAFs averaged 87.8 ± 4.0 % and were not significantly influenced by preload ($p = .370$) or gender ($p = .134$) (Table 3.1A).

Inspection of the IRFs indicated that the dynamics of the trunk disturbed by small random force impulses could be represented by an underdamped second-order system (Fig. 3.3A-B). It is clear by inspection of the IRFs and the superimposed second-order least-mean-squares fits that a second-order model provides an excellent description of the linear trunk dynamics. This was validated numerically by determining the second-order fit accuracy. Fit accuracy averaged 96.0 ± 4.3 % and was not significantly influenced by preload ($p = .333$) or gender ($p = .808$) (Table 3.1B).

The mean value of effective stiffness was 2.78 ± 0.96 N/mm and effective stiffness increased significantly with preload ($p < .001$). There was a 52.7 % increase in effective stiffness (2.20 to 3.36 N/mm) from the lowest preload level to the highest

Table 3.1A-B. Displacement VAF (A) and second-order fit accuracy (B) for each gender and preload condition. Gender and preload did not have an effect on VAF or fit accuracy as there was no significant statistical difference between the values at any of the conditions.

A		**VAF (%)**			
		100 N	**135 N**	**170 N**	**Mean**
	Males	85.6 (4.6)	87.0 (4.8)	88.1 (2.7)	**86.9 (4.1)**
	Females	88.7 (4.6)	87.9 (3.9)	89.2 (2.3)	**88.6 (3.7)**
	Mean	**87.2 (4.8)**	**87.4 (4.3)**	**88.7 (2.5)**	**87.8 (4.0)**
B		**Fit Accuracy (%)**			
		100 N	**135 N**	**170 N**	**Mean**
	Males	96.1 (3.8)	96.8 (2.7)	95.9 (3.7)	**96.3 (3.3)**
	Females	96.4 (3.2)	96.8 (2.3)	96.6 (2.2)	**96.6 (2.5)**
	Mean	**96.2 (3.4)**	**96.8 (2.4)**	**96.2 (2.9)**	**96.0 (4.3)**

(Table 3.2A). Effective stiffness did not vary with gender ($p = .425$) and there was no significant gender-by-preload interaction ($p = .101$).

The mean effective damping was 314 ± 72 N-s/m (Table 3.2B). Damping increased 24.8 % (274 to 342 N-s/m) from the lowest level of preload to the highest ($p < .001$). There was no significant main effect of gender in damping ($p = .360$), and no significant gender-by-preload interaction in damping ($p = .285$).

Table 3.2A-B-C. Measured effective stiffness (A), effective damping (B), and effective mass (C) for each gender and preload condition. There were no main effects for gender or any significant gender-by-preload interactions. Mean values with similar superscripts were not significantly different (p > 0.05)

A) Stiffness (N/mm)		**100 N**	**135 N**	**170 N**	**Mean**
	Males	2.20 (0.68)	2.62 (0.72)	3.07 (0.97)	**2.63 (0.85)**
	Females	2.20 (0.61)	2.91 (0.96)	3.62 (1.06)	**2.91 (1.05)**
	Mean	**2.20 (0.63)** ^{A}	**2.77 (0.85)** ^{B}	**3.36 (1.03)** ^{C}	**2.78 (0.96)**
B) Damping (N-s/m)		**100 N**	**135 N**	**170 N**	**Mean**
	Males	269 (68)	310 (84)	322 (67)	**300 (74)**
	Females	279 (50)	338 (64)	360 (69)	**326 (69)**
	Mean	**274 (58)** ^{A}	**325 (74)** ^{B}	**342 (69)** ^{B}	**314 (72)**
C) Mass (kg)		**100 N**	**135 N**	**170 N**	**Mean**
	Males	42.0 (8.1)	45.4 (5.9)	43.7 (6.7)	**43.7 (6.9)**
	Females	28.9 (5.5)	31.5 (6.6)	32.3 (7.6)	**30.9 (6.6)**
	Mean	**35.1 (9.5)** ^{A}	**38.1 (9.4)** ^{A}	**37.7 (9.1)** ^{A}	**37.0 (9.3)**

The mean effective trunk mass was 37.0 ± 9.3 kg (Table 3.2C). Males had a significantly higher effective trunk mass than females ($p < .001$), and effective trunk mass did not vary with preload ($p = .098$).

3.5 Discussion

A method of calculating effective trunk stiffness has been implemented that is robust and accurate. Stochastic force perturbations were applied at the T10 level of the trunk, and linear time-domain deconvolution techniques were used to calculate the nonparametric IRF representing the trunk dynamics. These IRFs were able to predict an average of 87.8 ± 4.0 % of the measured trunk kinematic response to randomly applied forces. A linear second-order model provided a good description of the dynamic relationship between applied trunk force and displacement, and produced an average fit accuracy of 96.0 ± 4.3 % when superimposed on the IRF. In addition, the parameters (i.e., effective mass and effective stiffness) obtained were validated by connecting a known mass and a spring with known stiffness (2.38 N/mm) to the servomotor, and administering the same protocol and analysis methods that we developed for the subjects. Since the error in both stiffness and mass (0.022 N/mm, 0.87 kg) was much lower than the stiffness and mass standard deviations calculated for the subjects (0.96 N/mm, 9.3 kg), these techniques were deemed accurate.

Joint stiffness has been found to increase with increasing muscle activation in the ankle (Agarwal and Gottlieb, 1977; Hunter and Kearney, 1982), elbow (Zhang and Rymer, 1997), and in the trunk (Cholewicki et al., 2000; Gardner-Morse and Stokes, 2001; Bull Andersen et al., 2004). Therefore, we hypothesized that the method we developed for calculating effective trunk stiffness would show an increase in stiffness with steady-state preload. As expected, effective trunk stiffness increased 52.7 % (2.20 to 3.36 N/mm) from the lowest level of preload to the highest.

The mean value of stiffness in this study was 2.78 ± 0.96 N/mm and ranged from 1.30 to 6.06 N/mm in various subjects and preload conditions. Gardner-Morse and Stokes (2001) applied a 4 Hz sinusoidal force disturbance to the trunk and reported much higher trunk stiffness values in the range of 14.5 N/mm to 19.8 N/mm. Some of the discrepancy in stiffness values can be attributed to the lower preloads in the current study. Also, Gardner-Morse and Stokes (2001) neglected damping which, given the extensive set of musculature the trunk possesses, may provide a significant contribution to trunk dynamics. Finally, much of the discrepancy might be attributed to the frequency content of the input waveform which was applied for system identification purposes. Pseudorandom stochastic inputs excite the system with a very broad frequency spectrum allowing identification techniques to give relevant information within the system's functional frequency range. Sinusoidal inputs contain only a single frequency thus can only give relevant information within a very specific frequency band that may or may not be encountered in functional situations (Kearney and Hunter, 1990). The average damped natural frequency observed in our study was 1.17 ± 0.26 Hz, and the largest exhibited by any subject was 1.95 Hz. Based on this frequency content we advise that stiffness analyses of the trunk should apply a continuous frequency spectrum over a minimum range of 0-6 Hz.

Cholewicki (2000) and Bull Andersen (2004) applied transient step inputs of force to the trunk and calculated average effective stiffness values of 785 ± 580 N-m/rad and 297 ± 61 N-m/rad, respectively, when compared at equivalent preload levels in the range of 170-190 N. In our analysis we calculated an average linear effective stiffness at the 170 N preload level of 3.36 ± 1.03 N/mm. Since the average distance between S1 and

T10 for our subjects was 274 mm, our linear effective stiffness can be converted to a rotational effective stiffness of 253 ± 55 N-m/rad. This agrees with results of Bull Andersen (2004) but both the mean and standard deviation is lower than Cholewicki (2000). The step inputs applied to the trunk by Cholewicki (2000) were much larger than Bull Andersen or the perturbations of the current study which would result in a much larger change in equilibrium. This may illustrate the importance in maintaining an approximately constant equilibrium preload and may demonstrate the advantage of employing techniques which utilize pseudorandom stochastic inputs about a constant preload level.

Effective trunk damping was found to be 314 ± 72 N-s/m and to increase 24.8 % (274 to 342 N-s/m) from the lowest level of preload to the highest. Cholewicki (2000) reported a mean damping value of 42 ± 64 N-m-s/rad, and also found damping to increase with increasing preload. Bull Andersen (2004) reported damping values ranging between 9.1 – 35.8 N-m-s/rad. Conversion of our linear effective trunk damping to rotational effective trunk damping yields an average value of 27.5 ± 9.0 N-m-s/rad. This agrees well with Bull Andersen, but is lower than Cholewicki (2001). Much like the variance in effective stiffness, the variance in effective damping observed in the Cholewicki study was much higher than Bull Andersen or the present study.

The increase in joint damping with preload has been shown not to be as large as the corresponding increase in joint stiffness. In fact, the increase in joint stiffness tends to match the increase in joint damping in such a way as to maintain a constant damping ratio, $\zeta = \frac{1}{2}\frac{b}{\sqrt{mk}}$ (Kearney and Hunter, 1990). Calculation of ζ in our study yielded a mean value of 0.512 ± .121 which, as expected, did not vary with preload ($p = .788$).

Since the trunk demonstrates a damping ratio as high as 0.512, it is clear that damping plays a large role in trunk dynamics. In fact if one were to neglect damping, effective stiffness may be underestimated by 33%.

The average effective trunk mass in our study was 37.0 ± 9.3 kg, and did not vary with the preload. Males (43.7 ± 6.9 kg) exhibited a significantly higher effective trunk mass than females (30.9 ± 6.6 kg). Each subject's effective trunk mass was roughly half of their total body mass which is to be expected since the trunk loading occurred at T10 close to the trunk center of mass. Gardner-Morse and Stokes (2001) reported a mean effective mass value of 14.1 kg, and their effective mass increased significantly with preload. They attributed these results to the non-rigid mass coupling of the upper body segments. It is well documented that joint inertia or effective mass should remain independent of joint torque (Agarwal and Gottlieb, 1977; Hunter and Kearney, 1982). Our results agree that effective trunk mass should be invariant with preload and also indicate that the effects of the non-rigid mass coupling of the upper body segments are small enough that effective trunk mass should remain close to the mass of the upper body.

The parameters of muscle dynamics are known to vary with the operating point of the joint determined by the mean level of torque, the perturbation amplitude, the mean joint position, and the level of agonist-antagonist co-contraction (Kearney and Hunter, 1990). This is indicative of a nonlinear system yet we employed a linear model to determine the trunk dynamics. The linear assumption can be made as long as the mean level of torque is held constant and the perturbation amplitude is kept relatively small so as to stay within one particular operating state of the muscles surrounding the joint.

Therefore, any comprehensive model of trunk stiffness must account for these nonlinearities using very small amplitude motion and by varying the mean level of muscle torque in small increments that encompass the entire range of muscular contraction levels. Therefore, the trunk dynamics reported in this study are valid only in the range of preload levels that were applied. The results should not be extrapolated to other levels of muscular activation or displacement amplitudes.

Although this method proved capable of accurately measuring the effective stiffness of the trunk within the trunk operating range examined, it is not without limitations. Related to the protocol, 18 % of the trials were thrown out due to missing infrared diode data or poor displacement VAF. Also, the placement of the infrared diodes at S1 and T10 provided only an approximation of the lumbar tissue displacements because the exact distance change between lumbar soft tissues during extension is unknown. Also, by controlling force perturbations it is possible that although the level of force amplitude was closely regulated, these given forces may cause different magnitudes of motion response from subject to subject. This could mean that two subjects were analyzed at two different operating states, which may influence the muscular response and stiffness characteristics. Future studies will minimize these limitations by using stochastic position perturbations instead of force perturbations. This may provide an additional advantage of allowing the separation of effective stiffness into its intrinsic and reflexive components (Kearney et al., 1997). Future studies should also further investigate the effect that gender has on effective trunk stiffness, as well as other variables such as fatigue, perturbation amplitude, prolonged static flexion, and loading direction.

3.6 Acknowledgement

This research was supported in part by a grant R01 AR46111 from CDC / National Institute for Occupational Safety and Health. We wish to thank G. Slota and G. Kauffman for their assistance in data collection and formatting.

Chapter 4

Effects of Static Flexion-Relaxation on Paraspinal Reflex Behavior

Kevin P. Granata, Ph.D.

Ellen Rogers

Kevin Moorhouse, M.S.

Clinical Biomechanics 20 (2005) 16-24

Musculoskeletal Biomechanics Laboratories
Department of Engineering Science & Mechanics
School of Biomedical Engineering and Science
Virginia Polytechnic Institute & State University
219 Norris Hall (0219)
Blacksburg, VA 24061, *USA*

Address correspondence to: K.P. Granata, Ph.D.
Musculoskeletal Biomechanics Laboratories
Department of Engineering Science & Mechanics
School of Biomedical Engineering and Science
Virginia Polytechnic Institute & State University
219 Norris Hall (0219)
Blacksburg, VA 24061, *USA*
Granata@VT.edu

Keywords: Low-Back; Reflex; Flexion-Relaxation

4.1 Abstract

Background. Static trunk flexion working postures and disturbed trunk muscle reflexes are related to increased risk of low back pain. Animal studies conclude that these factors may be related; passive tissue strain in spinal ligaments causes subsequent short-term changes in reflex. Although studies have documented changes in the myoelectric onset angle of flexion-relaxation following prolonged static flexion and cyclic flexion we could find no published evidence related to the human reflex response of the trunk extensor muscles following a period of static flexion-relaxation loading.

Methods. Eighteen subjects maintained static lumbar flexion for fifteen minutes. Paraspinal muscle reflexes were elicited both before and after the flexion-relaxation protocol using pseudorandom stochastic force disturbances while recording EMG. Reflex gain was computed from the peak value of the impulse response function relating input force perturbation to EMG response using time-domain deconvolution analyses.

Findings. Reflexes showed a trend toward increased gain after the period of flexion-relaxation ($P<0.055$) and were increased with trunk extension exertion ($P<0.021$). Significant gender differences in reflex gain were observed ($P<.01$).

Interpretations. Occupational activities requiring extended periods of trunk flexion contribute to changes in reflex behavior of the paraspinal muscles. Results suggest potential mechanisms by which flexed posture work may contribute to low back pain. Significant gender differences indicate risk analyses should consider personal factors when considering neuromuscular behavior.

4.2 Introduction

Workers who undergo periods of static or cyclic trunk flexion have an increased risk of low back pain(Marras et al., 1993;Punnet et al., 1991). Biomechanical factors contributing to this risk may include excessive or cumulative spinal load(Kerr et al., 2001), ligament and disc strain(Dolan P. et al., 1994) and spinal instability(Omino and Hayashi, 1992). Active muscular recruitment and reflexes play a major role in both spinal and ligamentous load as well as spinal stability(Gardner-Morse and Stokes, 1998;Granata and Marras, 1995). However, neuromuscular activity may be disturbed by periods of static or cyclic strain in the spinal ligaments and discs(Jackson et al., 2001;Solomonow et al., 1999). A change in reflex response associated with flexed working postures may contribute to limitations in stabilizing control and risk of injury(Solomonow et al., 1998). The goal of this study was to quantify changes in reflex response associated with prolonged trunk flexion in healthy human subjects.

Flexed trunk postures can apply tensile strain to paraspinal muscles and passive viscoelastic tissues of the spine. Flexion-relaxation occurs during extreme lumbar flexion wherein strain of the passive tissues in the trunk and spine support the external flexion load thereby allowing deactivation of the trunk muscles(Kippers and Parker, 1984). Prolonged passive stretch of skeletal muscles influences gamma motor-neuron drive to reduce muscle spindle excitability. *Studies* in the ankle joint document reflex inhibition following static and cyclic stretch loading(Avela et al., 1999;Rosenbaum and Hennig, 1995). Flexion strain in the ligaments may also influence reflex behavior. Flexion loading of the ligamentous tissues of the spine causes inter-vertebral laxity; specifically tissue creep and stress-relaxation. These effects have been quantified in human cadaveric

tissue(Twomey and Taylor, 1982), animal models(Solomonow et al., 2001), and in-vivo human measurements(McGill and Brown, 1992). Existence of reflex pathways have been observed originating from spinal ligaments to surrounding muscles; specifically the multifidus and longissimus(Kang et al., 2002). Thus, a perturbation force applied to the trunk causes transient tissue strain and excitation of large mechanoreceptors (Golgi, Pacinin, Ruffini fibers) in the spinal ligaments as well as type Ia and type II afferent muscle spindle sensors to initiate reflexive action of the paraspinal muscles(Simon, 1994). Biomechanical laxity of the spine from prolonged trunk flexion may influence neuro-sensor strain and reflex in response to force perturbations(Jackson et al, 2001). Therefore, changes in reflex response following prolonged strain of the spinal ligaments may be related in part to ligament laxity(Solomonow et al, 1999). Although studies have documented changes in the myoelectric onset angle of flexion-relaxation following prolonged static flexion and cyclic flexion (Dickey et al., 2003;Solomonow et al., 2003a), we could find no published evidence related to the human reflex response of the trunk extensor muscles following prolonged passive stretch.

To date, studies linking reflex disturbances to prolonged spinal flexion are limited primarily to animal models(Claude et al., 2003). In surgical preparations a mechanical strain was applied to feline supraspinal ligaments and the electromyographic response was observed in adjacent paraspinal muscles(Solomonow et al, 1998). Following repeated ligament strain a brief period of reflex hyper-excitability was observed(Jackson et al, 2001). However, this period of hyper-excitability was short lived. Ligament laxity caused the mechanoreceptors to become desensitized thereby inhibiting electromyographic response of the paraspinal muscles for many hours(Gedalia et al.,

1999). This laxity and disturbed reflex behavior may influence spinal stability(McGill and Brown, 1992). However, we could find no studies that validate these trends in humans. It is necessary to establish whether similar effects are observed from flexion-relaxation postures in humans.

To quantify changes in reflex response, System identification techniques can be applied to determine the myoelectric response attributable to a force perturbation, i.e. reflex amplitude is represented in terms of the amplitude and temporal characteristics of the impulse response(Zhang et al., 1999). This measurement technique was applied to quantify the reflex response from measured electromyography (EMG) from the paraspinals before and after a period of static flexion-relaxation in healthy human subjects. Based on the available literature we hypothesized that prolonged flexion-relaxation in healthy subjects influences paraspinal reflex response behavior.

4.3. Methods

4.3.1. Subjects

Eighteen subjects, with no previous history of low back pain participated after signing informed consent approved by the institutional review board at Virginia Tech. Subjects included nine females with mean (standard deviation) height 164.8 (7.2) cm. and weight 61.1 (9.6) kg, and nine males with mean height 183.1 (7.4) cm. and mean weight 75.9 (9.2) kg.

4.3.2. Protocol

Muscle recruitment, reflex gain, and perturbation kinematics were quantified before and immediately following a fifteen minute period of static passive flexion loading of the spine. To impose spinal ligament strain subjects sat on the floor with their trunk in full lumbar flexion and legs extended with a small padded bolster under the knees to reduce hamstring stretch and to tilt the pelvis posteriorly. They relaxed in this flexed posture while observing EMG from the erector spinae displayed on an oscilloscope to assure voluntary de-recruitment of the erector spinae, i.e. flexion-relaxation. Immediately following the flexion-relaxation period neuromechanical measurements of muscle recruitment, reflex gain and perturbation kinematics were repeated.

To record muscle response and kinematic behavior subjects stood upright with their pelvis and legs strapped to a rigid support (Figure 4.1). A harness and cable system attached the subject to a servomotor (Pacific Scientific, Rockford, IL*, USA*) such that cable tension applied flexion loads at the T10 level of the trunk. The motor was

programmed to provide three levels of isotonic preload, 100 N, 135 N, and 170 N. Superimposed on the preload were force perturbations of ±75 N applied in a pseudo-random stochastic fashion (Figure 4.2a) with a flat bandwidth from 0-10 Hz. Pseudorandom stochastic inputs were chosen to avoid voluntary responses from predictable stimuli(Kearney and Hunter, 1990). The applied forces were measured by a force transducer attached to the motor sampled at 1000 Hz (Omega, Stamford, CT*, USA*). Three pseudorandom perturbation trials of ten seconds each were performed at each preload level presented in random order before and after the flexion-relaxation protocol. After flexion-relaxation, some recovery may have occurred during the data collection trials. Statistical order effects were minimized by the trial randomization. Furthermore, only three minutes were required for data collection which was well below the documented recovery time constant, 9.4 minutes, reported by McGill and Brown (McGill and Brown, 1992).

EMG was recorded from bipolar surface EMG electrodes (Delsys, Boston, MA, USA) on the left and right rectus abdominus, internal oblique, external oblique, and erector spinae with placement as described by Marras(Marras and Mirka, 1992). EMG data were band-pass filtered in hardware between 20 and 450 Hz and sampled at 1000 Hz. The EMG signals were rectified and filtered using a 25 Hz, low-pass, seventh-order Butterworth filter in post-processing software (Figure 4.2b). Measured EMG data were normalized with respect to maximum voluntary exertion (MVE) in isometric trunk flexion, extension, combined torsion and extension, and combined torsion and flexion, recorded prior to the experiment. Trunk kinematics in response to the perturbation forces were recorded using surface mounted infrared motion sensors (Northern Digital,

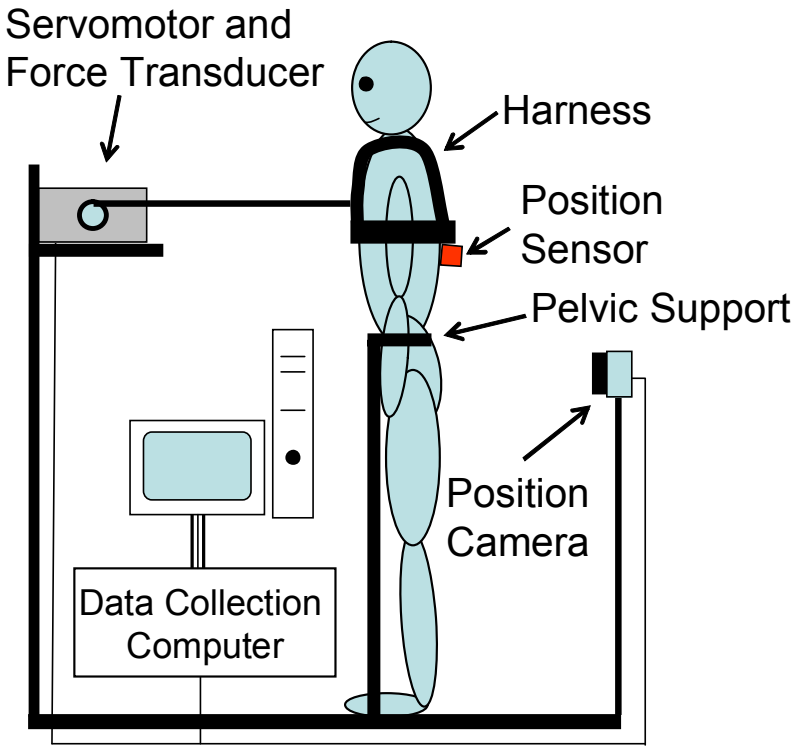

Figure 4.1. Experimental setup. Subject connected to servomotor for data collection.

Waterloo, Ontario, Canada). Sensors were placed over the subject's spinous processes at S1, L5, T10 and C7 and sampled at 100 Hz Figure 4.2c). Kinematic data were filtered using a 25 Hz, low-pass, seventh-order Butterworth filter in post-processing software (Matlab, Natick, MA*, USA*).

4.3.3. Analysis

Reflex response was quantified in terms of latency and gain from the erector spinae EMG. A nonparametric impulse response function (IRF) was calculated from the

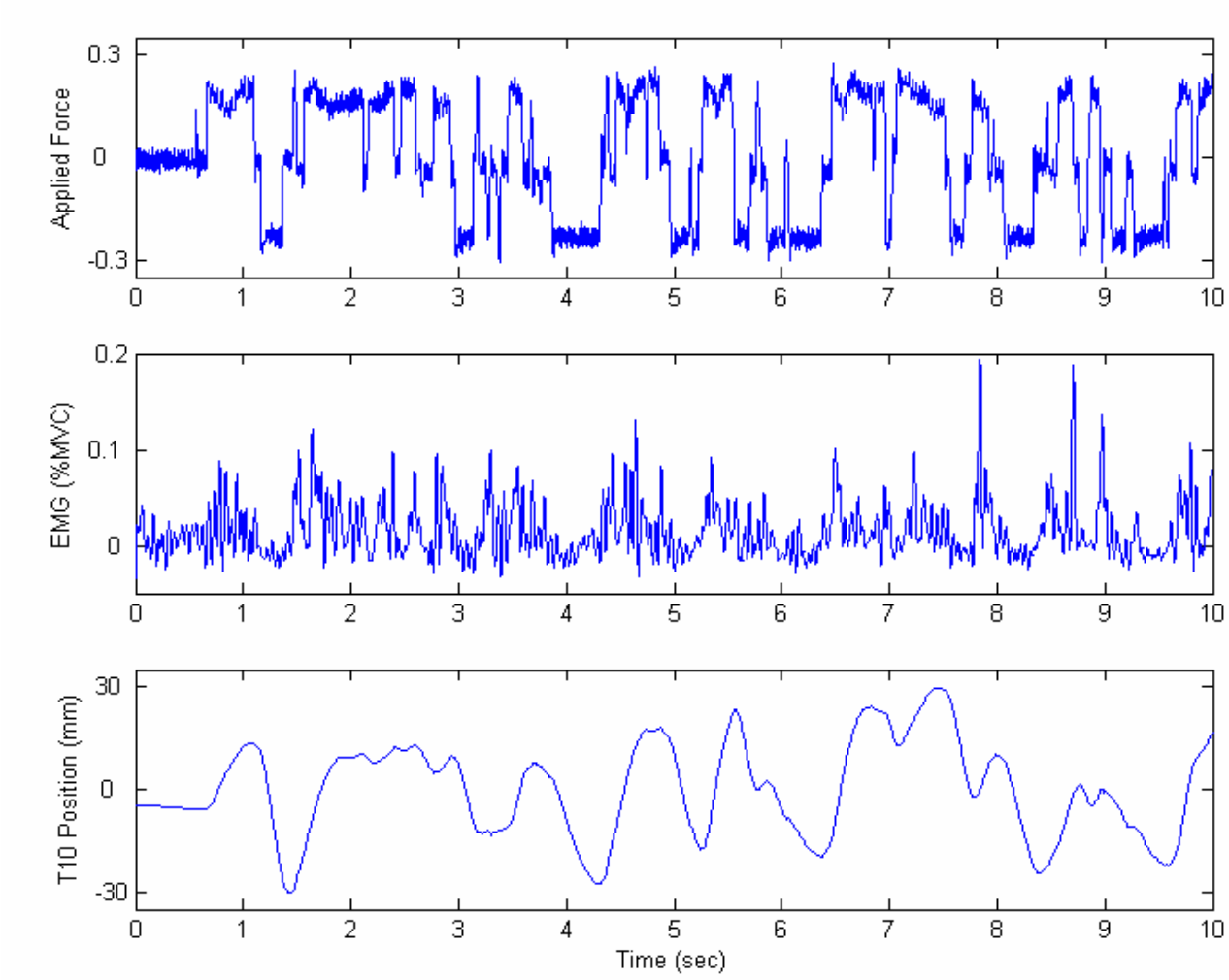

Figure 4.2. Force input, erector spinae EMG output and trunk movement in a female subject after the flexion protocol.

pseudorandom force input and the rectified EMG output of the erector spinae muscles. Calculation of the nonparametric IRF was based on deconvolution techniques for a time-delayed linear systems response(Mirbagheri et al., 2000). For any linear time-invariant (LTI) system, the output y(t), i.e., rectified EMG, can be described by the impulse response function h(t) of the system convolved with (notated *) the applied input signal, x(t), i.e. external trunk force,

$$y(t) = \int_{T_1}^{T_2} h(\tau)x(t-\tau)dt = h(t) * x(t) \tag{4.1}$$

where the $h(\tau)$ is considered trivial for time lags $\tau<T_1$ and $\tau>T_2$. Using this property, any LTI system can be described in its entirety by its IRF because once h(t) is known, the output of the system can be determined for any input. Accordingly, the discrete-time impulse response function can be represented in terms of the input autocorrelation function and the input/output cross-correlation function:

$$c_{xy}(k) = \Delta t \sum_{j=M_1}^{M_2} h(j)c_{xx}(k-j) \tag{4.2}$$

where the input and output are sampled every Δt seconds, $M_1 = \frac{T_1}{\Delta t}$ and $M_2 = \frac{T_2}{\Delta t}$. This equation can then be written in matrix form as:

$$C_{xy} = \Delta t\, C_{xx}\, H \tag{4.3}$$

where C_{xy} is an $M_2 - M_1 + 1$ length vector whose i^{th} element is $c_{xy}(M_1 + i - 1)$, C_{xx} is an $M_2 - M_1 + 1$ square matrix whose i, j^{th} element is $c_{xx}(i - j)$ and H is an $M_2 - M_1 + 1$ length vector whose i^{th} element is $h(M_1 + i - 1)$. Using simple matrix inversion one can solve for the impulse response function, H, representing the EMG response (Figure 4.3). After T_2=120 msec any response is considered to be arbitrarily voluntary and therefore not quantified as a reflex(Matthews, 1991).

Both the applied trunk force and the rectified EMG were scaled to yield a mean value of zero prior to analysis in order to ensure accuracy of correlation function estimations. Published techniques illustrate that adding white noise to the input signal reduces the effect of system noise by decorrelating the data sampling artifact from the

input signal(Ljung and Ljung, 1998). The magnitude of white noise added was 30% of one standard deviation of the input trunk force.

To measure the quality of the IRF representation of the reflex response, the computed IRF was convolved with the original pseudorandom force sequence to produce an estimate of the EMG signal. Root-mean-square (RMS) difference between the physiologic signal and the estimated signal was recorded as percent variance accounted for (VAF_{Reflex})(Hunter and Kearney, 1983). VAF_{Reflex} equal to 100% indicates that the IRF predicts exactly the measured EMG signal from the input force perturbations. Reflex gain, G_R, was determined from the peak amplitude of the IRF and the latency, t_R, was the time at which the maximum peak occurred (Fig. 4.3). For this analysis a reflex response was defined as a peak occurring two standard deviations or more above the mean IRF signal. If no peak was above this threshold the trial was discarded.

Since perturbation forces were applied in a random time sequence the trunk movement had random qualitative appearance (Figure 4.2c). To quantify movement amplitude kinematic gain, G_K, was estimated from the peak of the IRF determined from the pseudorandom force input and the position output recorded from the infrared motion sensors (Figure 4.4). G_K represents the dynamic trunk flexion-extension movement in response to the force perturbations(Moorhouse and Granata, 2004). Analogous to the reflex data, VAF_K was computed to estimate the quality of the kinematic measurement.

Secondary analyses included quantification of baseline trunk muscle recruitment and pelvic angle. To quantify trunk muscle recruitment the RMS level of the normalized, rectified and filtered EMG signal from each muscle was quantified during the period of

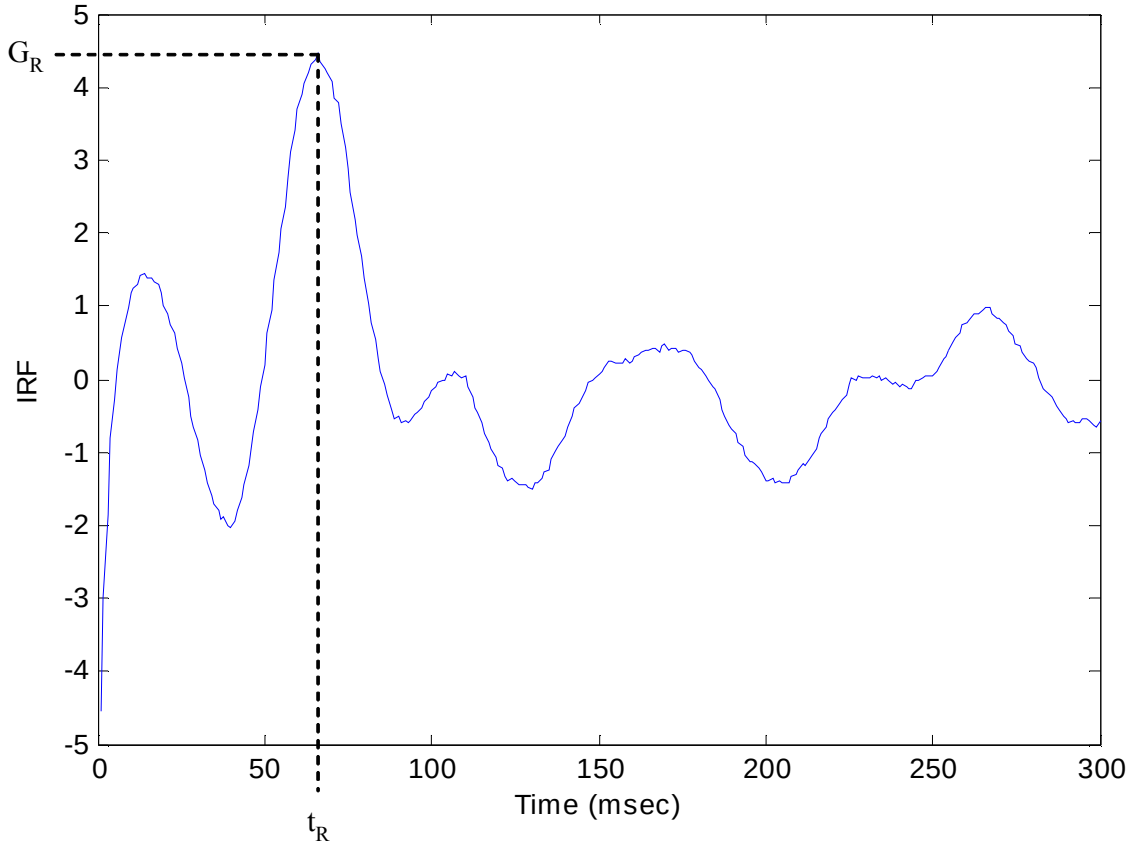

Figure 4.3. Impulse Response Function (IRF) for the erector spinae muscle in a female subject after the flexion protocol. The peak reflex gain and rise time are labeled.

constant isotonic load, i.e. 250 msec mean value recorded immediately before the initiation of the pseudorandom force perturbations. Although subjects maintained an upright trunk posture lumbar lordosis was not controlled. Pelvic angle was quantified as an analog to lordosis and measured from the angle between the two kinematic sensors placed at S1 and L5. This was recorded during the period of constant isotonic load prior to initiation of the pseudorandom force perturbations of each trial.

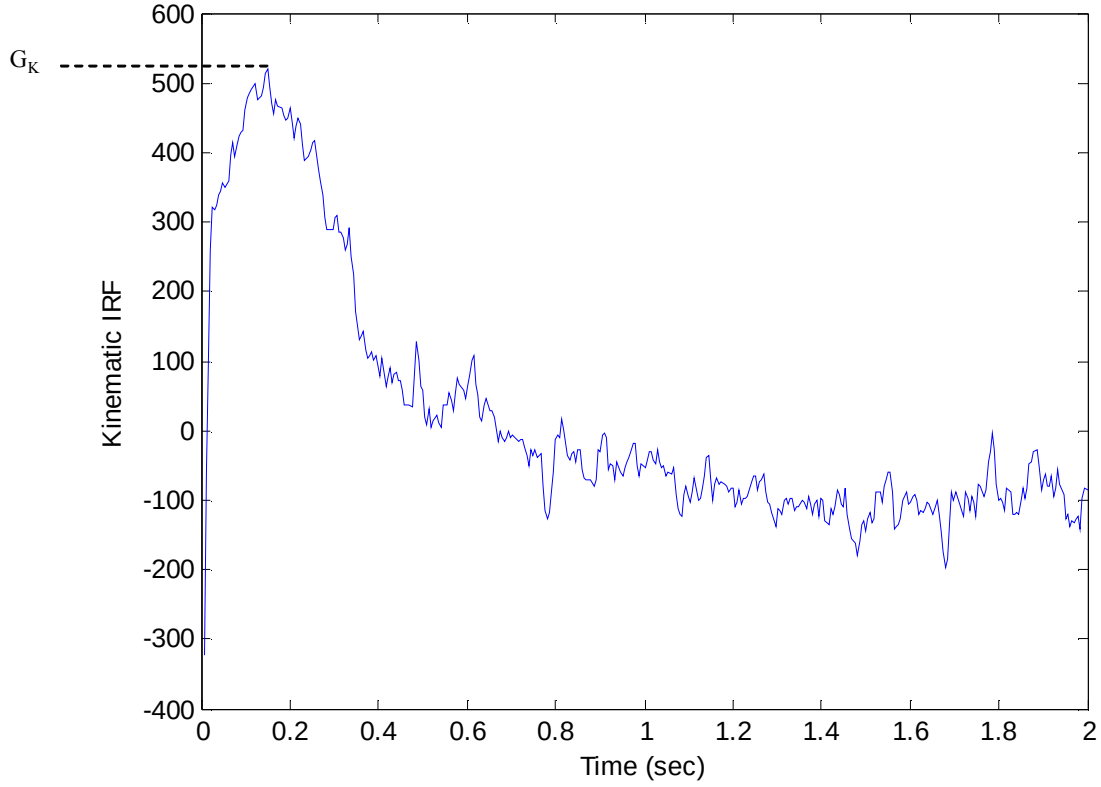

Figure 4.4. Impulse Response Function (IRF) relating input force perturbation to trunk movement in a female subject. Kinematic gain, G_K is labeled.

4.3.4 Statistical Analysis

Statistical repeated measures analyses (ANOVA) were performed to determine the effect of flexion-relaxation, gender and preload on baseline EMG activity, G_R, t_R, VAF_{Reflex}, G_K, and VAF_K. The independent variable of gender was analyzed as a between subject variable while flexion-relaxation effect and preload were analyzed as within subject variables. Significance was determined at the level of $\alpha<0.05$. Tukey honest significant difference post-hoc analyses were used to compare differences among significant treatments. To quantify representative changes in antagonistic coactivation

and lumbar lordosis the RMS EMG activity from the rectus abdominis and pelvic angle were similarly tested for influence of gender and flexion-relaxation.

4.4 Results

Reflexes were observed in 81.4% of the trials. There was no significant difference in rate of reflex occurrence for gender, flexion-relaxation effect or preload. VAF_{Reflex} had an average value of 48%. There were no significant main effects of gender, flexion-relaxation, or preload on VAF_{Reflex}. However, the effect of preload approached significance (P=0.056). This phenomenon is attributed to the fact that at higher preload levels EMG response is greater, resulting in a higher signal to noise ratio. At lower preloads the lower signal to noise ratio negatively affects the accuracy of the impulse response. VAF_K had an average value of 93%. There were no significant effects of flexion-relaxation, preload level, or gender on VAF_K.

Analyses revealed that reflex gains, G_R, were influenced significantly by flexion-relaxation, gender and preload as well as a significant gender-by-preload interaction (Tables 4.1 and 4.2). Three way interactions yielded no significance effects and therefore were not reported. Females had larger reflex G_R than males (P<0.01). Post-hoc analyses of the gender-by-flexion-relaxation interaction revealed that G_R was greater in females than in males after the flexion-relaxation protocol (P<0.0002) but the gender difference failed to reach statistical significance before the period of flexion-relaxation (P=0.19).

The main effect of flexion-relaxation in reflex gain was slightly outside the range of significance (P=0.055) with a trend suggesting an increase in G_R after flexion. Post-hoc analyses indicated a significant increase in G_R after flexion-relaxation (P<0.003) in females. Males had no significant change for the number of subjects tested.

Table 4.1. Effects of isotonic trunk extension preload. Mean (standard deviation) of peak reflex gain, latency, and kinematic gain. Results show significant main effects for gender, preload and two-way interactions on reflex gain, G_R, and kinematic gain, G_K.

		Men	Women	Average
Reflex Gain G_R (% / N)	100 N preload	0.987 (0.375) [3]	1.476 (0.846) [3]	1.224 (0.688) [2]
	135 N preload	1.032 (0.465) [3]	1.467 (0.735) [3]	1.259 (0.640)
	170 N preload	1.112 (0.418) [3]	1.644 (0.834) [3]	1.370 (0.726) [2]
	Average	1.054 (0.420) [1]	1.529 (0.802) [1]	1.285 (0.677)
Reflex Latency t_R (msec)	100 N preload	70.70 (17.71)	68.36 (12.07)	69.56 (15.17)
	135 N preload	68.46 (15.93)	65.45 (7.59)	67.00 (12.59)
	170 N preload	66.71 (13.85)	63.62 (9.17)	65.21 (11.83)
	Average	68.62 (15.84)	65.81 (9.89)	67.26 (13.33)
Kinem. Gain G_K (mm / N)	100 N preload	590.4 (90.83) [4]	582.4 (85.70) [4]	598.5 (87.8) [2]
	135 N preload	557.5 (74.49)	558.6 (73.34) [4]	558.0 (72.9) [2]
	170 N preload	521.6 (87.88) [4]	511.6 (89.34) [4]	517.2 (87.4) [2]
	Average	556.5 (87.93)	559.6 (90.62)	557.9 (88.73)

[1] significant main effect for gender $P<0.05$

[2] significant main effect for preload $P<0.05$

[3] significant effect of gender within preload level $P<0.05$

[4] significant effect of preload within gender group $P<0.05$

Reflex gain increased with preload. A significant difference in G_R occurred between the lowest and highest preload settings ($P<0.02$), with reflex gain, G_R, being greater at higher preloads. There was also a significant gender difference in G_R at each preload level, with G_R being greater in women than men. There was no significant difference in reflex latency, t_R, due to preload, gender, or flexion-relaxation protocol.

Table 4.2. Effects of flexion-relaxation (FR). Mean (standard deviation) of peak reflex gain, latency, and kinematic gain. Interactions between variables of gender, flexion-relaxation effect, and preload are shown. Significances are indicated by superscripts identified in footnotes.

		Men	Women	Average
Reflex Gain G_R (% / N)	Before FR	1.070 (0.469)	1.333 (0.635) [4]	1.198 (0.569) [2]
	After FR	1.038 (0.369) [5]	1.724 (0.905) [4 5]	1.371 (0.763) [2]
	Average	1.054 (0.420) [1]	1.529 (0.802) [1]	1.285 (0.677)
Reflex Latency t_R (msec)	Before FR	69.39 (15.83)	65.36 (8.28)	67.43 (12.84)
	After FR	67.86 (15.97)	66.26 (11.33)	67.08 (13.87)
	Average	68.62 (15.84)	65.81 (9.89)	67.26 (13.33)
Kinem. Gain G_K (mm / N)	Before FR	562.1 (95.00)	581.1 (96.19) [4]	570.6 (95.10) [3]
	After FR	550.9 (81.47)	538.1 (81.01) [4]	545.2 (80.75) [3]
	Average	556.5 (87.93)	559.6 (90.62)	557.9 (88.73)

FR = Flexion-Relaxation

[1] significant main effect for gender $P<0.01$

[2] main effect for flexion-relaxation approaching significant $p = 0.055$

[3] main effect for flexion-relaxation significant $P< 0.01$

[4] significant effect of flexion-relaxation within gender group $P<0.05$

[5] significant effect of gender within flexion-relaxation condition $P<0.05$

There was a significant main effect of flexion-relaxation in kinematic gain with G_K being reduced after flexion-relaxation ($P<0.003$). There was no significant difference in G_K between males and females. However, gender-by-flexion-relaxation interactions revealed a significant effect due to flexion-relaxation in females ($P<0.011$). There was no significant effect of flexion-relaxation in males for G_K ($P=0.72$). There was a

significant main effect of preload on G_K, with the highest G_K occurring at the lowest preload.

Effects of gender and flexion-relaxation on baseline muscle activity and pelvic angle were evaluated (Table 4.3). Rectus abdominis coactivation was greater in females than in males both before and after flexion-relaxation ($P<0.001$). In females the baseline rectus abdominis coactivation showed no significant change due to flexion-relaxation. In males, there was a trend toward increased coactivation following flexion-relaxation ($P=0.070$). Pelvic angle increased following flexion-relaxation ($P<0.002$). A significant gender-by-flexion-relaxation interaction revealed that the change was significant in males ($P<0.024$), but not in female participants ($P=0.23$). There was no main effect of gender in pelvic angle.

Table 4.3. Mean (standard deviation) of baseline rectus abdominis activity and pelvic angle.

		Men	Women	Average
Rectus Abd EMG (%MVC)	Before FR	0.0336 (0.0603) [2]	0.0752 (0.1684) [2]	0.0544 (0.1276)
	After FR	0.0467 (0.0888) [2]	0.0709 (0.1691) [2]	0.0588 (0.1351)
	Average	0.0402 (0.0758)	0.0731 (0.1681)	0.0566 (0.1311)
Pelvic Angle (deg)	Before FR	12.49 (7.65) [3]	13.97 (6.51)	13.10 (7.03) [1]
	After FR	14.42 (8.08) [3]	15.51 (5.95)	14.87 (7.09) [1]
	Average	13.45 (7.72)	14.74 (6.05)	13.98 (7.01)

FR = Flexion-Relaxation

[1] significant main effect for flexion-relaxation $P<0.05$

[2] significant effect of gender within flexion-relaxation condition $P<0.05$

[3] significant effect of flexion-relaxation within gender group $P<0.05$

4.5. Discussion

Four primary effects were observed in the results. First, trends indicated higher reflex gain following a period of static flexion-relaxation, specifically in females. This indicates greater EMG response per unit of perturbation force, i.e. hyper-excitable paraspinal reflex response following 15 minutes of flexion-relaxation. Second, reflex gain increased with trunk flexion preload. Third, females exhibited larger reflex gains than males. Finally, kinematic gain decreased following flexion-relaxation indicating less trunk movement in response to a force perturbation.

Matthews(Matthews, 1991) showed that the human stretch reflex consists of at least two different components including a short latency spinal reflex and a long latency transcortical reflex. The short latency reflex, occurring between 10-30 msec was observed in some trials (Figure 4.3) but the amplitude was smaller than the peak G_R and therefore not included in the statistical analyses. Peak amplitude of the long latency reflex was represented by the reflex gain, G_R, of the IRF and typically occurs around 60 msec(Matthews, 1991). This accounts for conduction time from the spindle and mechanoreceptors, through a multi-synaptic reflex loop and back to the muscle as well as propagation time of the muscle action potentials. Magnusson et al.(Magnusson et al., 1996) noted that sudden flexion loading and unloading of the trunk yielded mean reflex delays of 100 msec and 50 msec respectively. Thus, experimental protocol may be an important factor when examining reflex latency. In the current study the perturbation loading was stochastic and included both flexion loading and flexion unloading with mean reflex latency t_R = 67 msec. Reflex latency, t_R, showed no significant effects for

gender, flexion-relaxation or preload level. However, the response rate was fast enough that it may contribute to control of the trunk in response to external force disturbances.

Trends toward increased reflex gain, G_R, were observed following 15 minutes of static flexion-relaxation posture ($p=0.055$). Passive stretch of skeletal muscles can reduce muscle spindle excitability thereby inhibiting reflex amplitude(Avela et al, 1999;Rosenbaum and Hennig, 1995). Conversely, animal models demonstrate that passive stretch of spinal ligaments can cause brief hyper-excitability of the paraspinal muscle response(Solomonow et al., 2003b). Our results suggest similar behavior is observed in humans. The force sequences before and after the flexion-relaxation protocol were similar in amplitude and signal character. However, this does not guarantee similar movement dynamics. Kinematic response to the force perturbations, G_K, was reduced following 15 minutes of static flexion-relaxation. Hence, the force disturbance caused less trunk movement after the flexion-relaxation protocol than before. This was contrary to our expectations because published data suggest reduction in stiffness following prolonged flexion-relaxation(McGill and Brown, 1992;Solomonow et al, 2003a) suggesting increases in G_K should be expected. An increase in baseline muscle contraction could partially explain the reduced G_K values after flexion-relaxation. However, no changes in baseline EMG levels were observed in the data. It should be noted that a change in G_K was significant only in the female participants. Similarly, the increase in reflex gain, G_R, was significant only in the female participants. Thus, we believe that the decrease in movement following flexion-relaxation may be attributed to the increase in reflex gain. Recognizing that the natural kinematic frequency of the trunk is approximately 1 Hz (Figure 4.4) the reflex response can contribute as feedback control

to limit movement following an external force disturbance. This suggests that paraspinal reflexes may play a significant role in the control of trunk muscle stiffness and associated spinal stability. In animal models brief periods of hyper-excitable reflexes after flexion-relaxation was followed by prolonged periods of reflex depression that may limit spinal stability(Claude et al, 2003;Jackson et al, 2001;Solomonow et al, 1999). Further research is necessary in human subjects to determine whether reflex inhibition is observed following the period of hyperexcitability associated with prolonged flexion-relaxation.

Reflex gain increased with trunk extension effort. Motor neurons that initiate the reflex action are influenced by muscle tone and may not be excited if the muscle is completely relaxed(Matthews, 1986). Therefore, research shows that reflex excitation increases with low-level preactivation of muscles whereas at high exertion levels muscle stiffness is increased thereby causing reduced displacement and reflex response(Bennett et al., 1994;Matthews, 1986). The saturation point between enhanced reflex excitability and reduced response is generally considered to be approximately 50% of maximum voluntary contraction. During trunk extension exertions Stokes et al.(Stokes et al., 2000) showed that muscle responses occurred less frequently at high preloads than at low exertion levels. In the current study, mean distance from the L5/S1 junction to the level of T10 where the force perturbation was applied was 14.9 cm indicating that the three preloads were equivalent to external flexion moments of 14.9 N-m, 20.1 N-m, and 25.3 N-m. These are less than 20% of the maximum extension moment strength reported by Parnianpour(Parnianpour et al., 1991). Because the effort levels were below 50% MVC, one should expect increased reflex gain with increased preload. Thus, results were

consistent with the neurophysiologic literature, i.e. for the three preload levels tested reflex gain increased significantly from the lowest to the highest level.

Reflex gain was greater in females than males. Since force perturbations of 75 N were applied to both males and females alike, one might expect that the smaller trunk inertia of the women would result in greater movement and subsequently larger G_K. This was not observed. However, we have noted elsewhere that trunk stiffness is greater in females than in males (Moorhouse and Granata, 2004). Increased stiffness combined with smaller inertia causes high natural frequency of motion indicating faster movement in females. The reflex response is strongly influenced by tissue strain rate(Simon, 1994). An estimate of the measured EMG response was achieved by convolving the reflex IRF with the measured input force signal for comparison with the actual EMG signal. The variance-accounted-for (VAF) by the IRF explained approximately half of the EMG signal in the current study. This demonstrates the ability to identify reflex behavior from force perturbations. It also highlights a limitation of the study, i.e. further efforts must attempt to reduce the variability of the reflex gain estimate. Mirbagheri et al.(Mirbagheri et al, 2000) concluded that VAF of the reflex response may exceed 95% if one uses kinematic velocity as the reference disturbance rather than the external force signal examined in the current study. Hence, future research must quantify the paraspinal muscle reflex response with respect to trunk kinematics. Nonetheless, if the force disturbance produced faster initial kinematic disturbances in the female participants then greater reflex gain should be expected. This has been observed in the knee joint and may explain the gender-specific behavior observed in our data(Shultz et al., 2004). We believe this velocity-dependent contribution to increased reflex gain in women helped to

limit movement amplitude following the external force disturbances and explains why G_K was similar in men and women. Further study is necessary to understand gender specific neuromuscular control behaviors that may influence spinal stability.

Several effects remain unexplained. Why was the change in reflex gain following flexion-relaxation observed only in females? As noted above, we believe a gender difference in trunk stiffness may contribute to reflex gain but this fails to explain why flexion-relaxation caused a change in neither G_R nor G_K in male subjects. It is possible that mechanical and neuromuscular response to flexion-relaxation postures is gender specific. Published studies indicate that females developed more spinal laxity than males during static flexion-relaxation protocols(McGill and Brown, 1992;Solomonow et al, 2003a). Nonetheless, those studies report significant increases in trunk laxity and associated tissue creep in males. Hence, we expected change in reflex in the males as well as in females. Trunk muscle co-contraction may contribute to gender effects. Our results agree with previous measurements wherein gender differences in antagonistic coactivity of the trunk muscle have been observed(Granata et al., 2001). There was no change in baseline EMG following flexion-relaxation in either males or females (Table 4.3) but the male participants demonstrated a trend toward greater antagonistic coactivation after flexion-relaxation than before ($P<.07$). Spinal posture may also influence reflex gain by modulating the muscles and ligament strain lengths. Although all subjects maintained an upright trunk posture both before and after the flexion-relaxation protocol, pelvic tilt angle increased following flexion-relaxation in male subjects suggesting greater lumbar lordosis. No change in posture was observed in the female subjects. The combined effects of co-contraction and spinal curvature may

influence gender-specific response to flexion-relaxation postures. Gender differences in reflex response to the flexion-relaxation protocol may suggest complex neuromotor and biomechanical mechanisms, and may indicate potential gender differences to injury risk from static flexion work postures.

In conclusion, paraspinal reflexes demonstrated a trend toward increased reflex gain immediately following 15 minutes of static flexion-relaxation posture. These results agree with animal models wherein a hyper-excitable reflex response is observed following prolonged ligament stretch(Solomonow et al., 2003c). It is noteworthy that those feline models demonstrate that the period of hyper-excitability is brief and followed by a prolonged reflex depression lasting up to 7 hours. The current study did not record the recovery of the reflex gain so it remains to be demonstrated whether reflex depression is observed in humans following flexion-relaxation. These changes in reflex response may influence stability control and risk of low-back pain. Patients with low-back pain demonstrate reduced and slowed reflexes compared to asymptomatic control subjects(Luoto et al., 1996;Radebold et al., 2000) but it remains unclear whether this is a compensatory consequence of low-back pain(Van Dieen et al., 2003) or a contributing cause. Nonetheless, it has been proposed that changes in paraspinal muscle response following flexed posture work may contribute to LBP risk(Holm et al., 2002). Results suggest that occupational activities that require prolonged trunk flexion may contribute to changes in reflex behavior of the paraspinal muscles. Results also indicate that risk analyses must consider personal factors including gender when considering neuromuscular behavior that influence spinal load and stability.

4.6 Acknowledgement

This research was supported in part by a grant R01 AR46111 from NIAMS of the National Institutes of Health. We wish to thank G. Slota and G. Kauffman for their assistance in data collection and formatting.

Chapter 5

The Role of Intrinsic and Reflexive Dynamics in the Control of Spinal Stability

To be submitted for publication

Kevin M. Moorhouse, M.S.

Kevin P. Granata, Ph.D.

Musculoskeletal Biomechanics Laboratories
Department of Engineering Science & Mechanics
School of Biomedical Engineering and Science
Virginia Polytechnic Institute & State University
219 Norris Hall (0219)
Blacksburg, VA 24061

Address all correspondence to:

K.P. Granata, Ph.D.
Musculoskeletal Biomechanics Laboratories
Department of Engineering Science & Mechanics
School of Biomedical Engineering and Science
Virginia Polytechnic Institute & State University
219 Norris Hall (0219)
Blacksburg, VA 24061
Phone: (540) 231-5316
FAX: (540) 231-4547
Granata@VT.edu

5.1 Abstract

Spinal stability describes the ability of the neuromuscular system to maintain equilibrium in the presence of kinematic and control variability, and may play an important role in the etiology of low-back disorders (LBDs). Spinal stability is related to the recruitment and control of active muscle stiffness which has both intrinsic and reflexive components. A nonlinear parallel-cascade system identification analysis technique was implemented to separate overall trunk stiffness into intrinsic and reflexive components. Eleven healthy adult male subjects stood upright in a pelvic restraint structure with a harness and rod system attaching the T10 level of the subject to a servomotor programmed to apply pseudorandom position perturbations to the trunk. Prior to initiation of the perturbation sequence, subjects were instructed to equilibrate one of three pre-specified levels of isometric trunk extension exertion (20%, 35%, or 50% MVC) and the 20% MVC condition was performed at both minimal co-contraction and maximal co-contraction. Subsequent analysis was able to separate the intrinsic and reflexive components of trunk dynamics and predict the total trunk force resulting from the pseudorandom position perturbations with an accuracy of 80.9 ± 3.6 %. Mean proportional intrinsic response, P_{INT}, was –0.0219 ± 0.350 N/mm and increased significantly with both extension exertion level and co-contraction. Eight of the eleven subjects exhibited a negative value of P_{INT} indicating that the intrinsic muscle stiffness of the trunk alone was insufficient to stabilize the spine. Mean reflexive stiffness gain was 208 ± 34.5 N-m/s and increased significantly with extension exertion but did not vary with co-contraction. Results of this study indicate that any comprehensive spinal stability model should include the role of reflexes, as they may account for 75 % of the stabilizing dynamics of the torso.

5.2 Introduction

Reflex response may play an important role in the control of spinal stability. Stability describes the ability of the neuromuscular system to maintain equilibrium in the presence of kinematic and control variability. Panjabi describes three sub-systems that contribute to spinal stability (Panjabi, 1992a). One is the passive sub-system consisting of the spinal ligaments, discs and bone; the second is the active sub-system attributed to steady-state muscle recruitment; the third is the neural feedback sub-system that includes active and voluntary responses. The contribution of intervertebral disc and passive ligament stiffness to stability is considered minimal in neutral spinal postures (Panjabi, 1992b). Therefore, existing models and available biomechanical measurements focus on the intrinsic stiffness of active muscles as the primary control mechanism for spinal stability (Bergmark, 1989). The role of reflex dynamics for the control of spinal stability has been typically overlooked.

Intrinsic stiffness of active muscles contributes to the control of spinal stability. Stiffness is a subcomponent of the involuntary dynamics of the torso. It may be defined as the relation between a small perturbation force and involuntary change in posture. Torso stiffness is dominated by active muscles when in a near upright posture as studies have shown that passive trunk stiffness is small compared to trunk stiffness during active exertions (McGill et al., 1994; Moorhouse and Granata, 2005). Intrinsic stiffness is the component of active muscle stiffness that provides immediate restorative force in response to a postural disturbance; hence it does not include any mechanical contributions from the delayed paraspinal reflex response. The intrinsic stiffness of muscle contributes to the elastic energy stored in the musculoskeletal system (Cholewicki and McGill, 1996). This is important because static stability is achieved when the

equilibrium state of the spine is also a state of minimum potential energy (Thompson, 1984). The strain energy in the musculotendonous unit is related to recruitment activation. Specifically, intrinsic stiffness of active paraspinal muscle increases with steady-state contractile force and contributes to the bending stiffness and stability of the spinal column (Bergmark, 1989). However, to achieve spinal stability it is necessary to assume that the intrinsic muscle stiffness is sufficient to compensate for the gradient in gravitational moment at each vertebra (Gardner-Morse et al., 1995; Granata et al., 2001). It is unclear whether this assumption is true, i.e. whether the intrinsic stiffness of active muscles without reflex response is sufficient to achieve stability of the spine.

Reflex response can contribute to the apparent stiffness of active muscle. Paraspinal reflexes contribute to the overall dynamics of the trunk by responding to perturbation movements and associated muscle strain, i.e. active feedback control (Granata et el., 2004). Thus, reflexes provide restorative forces similar to intrinsic stiffness but are time-delayed by the reflex loop response latency. The combined behavior of the intrinsic muscle stiffness and the paraspinal reflex response is commonly referred to as the "effective stiffness" (Cholewicki et al., 2000). Estimates of muscle dynamics in the ankle indicate that up to 55 % of effective muscle stiffness may be attributed to reflexes (Mirbagheri et al., 2000). We are unaware of any study to quantify the reflex contribution to trunk stiffness.

Existing biomechanical models of spinal stability ignore the role of reflexes despite evidence suggesting that reflex response may play a role in the mechanics of low-back pain (LBP). LBP patients have been found to demonstrate abnormal reflex response including reduced reflex gain and slowed latency (Luoto et al., 1996; Hodges and

Richardson, 1996). Data from Radebold suggest that response dynamics for stabilizing control is impaired in LBP patients (Radebold, 2001). Therefore, it is necessary to characterize the role of reflexes in the control of spinal stability.

The goal of this study was to separate and quantify the intrinsic and reflexive components of trunk stiffness. Since reflex and intrinsic components of trunk stiffness coexist, most studies regarding joint dynamics lump them together (Cholewicki et al., 2000; Moorhouse and Granata, 2005). Initial attempts to isolate the reflex contribution to joint dynamics compared joint stiffness in animal models before and after surgically deafferentating the reflex pathways (Nichols and Houk, 1976; Hoffer and Andreassen, 1981). These techniques were impractical for in vivo study in human subjects. Hence, methods were developed to separate the intrinsic and reflexive contributions using system identification methods (Kearney et al., 1997; Zhang and Rymer, 1997; Mirbagheri et al., 2000). Therefore, in the current study we applied a PRBS of position perturbations to the trunk and implemented a nonlinear system identification technique to separate and quantify the intrinsic and reflexive components of effective trunk stiffness. It was hypothesized that the reflex response in the torso musculature is a necessary component of spinal stability.

5.3 Methods

5.3.1 Subjects

Eleven healthy male subjects (mean age 26.4 ± 2.7 yr, mean height 181.1 ± 8.0 cm, mean weight 82.2 ± 13.2 kg) with no previous history of low back pain participated after signing informed consent approved by the institutional review board at Virginia Tech.

5.3.2 Apparatus

Subjects stood upright in a pelvic restraint structure designed to restrict the motion of the lower body (Figure 5.1). A harness and rod system attached the subject to a geared DC servomotor (Pacific Scientific, Rockford, IL) in order to apply small postural disturbances to the torso. Unlike our previous studies wherein force disturbances were applied, in the current study the motor accurately controlled the small angle displacement positions of the torso (Figure 5.2A). Trunk displacement was measured with an optical encoder (1024 counts/rev resolution) attached to the servomotor shaft. Force was measured by means of an in-line force transducer (Omega TQ-401). Position and force signals were demeaned and filtered using a 75 Hz, low-pass, seventh-order Butterworth filter.

EMG was recorded using bipolar surface EMG electrodes (Delsys, Boston, MA, USA) over the left and right rectus abdominus, internal oblique, external oblique, and erector spinae with placement as described by Marras and Mirka (1992). Specifically, electrodes were secured to the skin as follows: the rectus abdominis were recorded 3 cm.

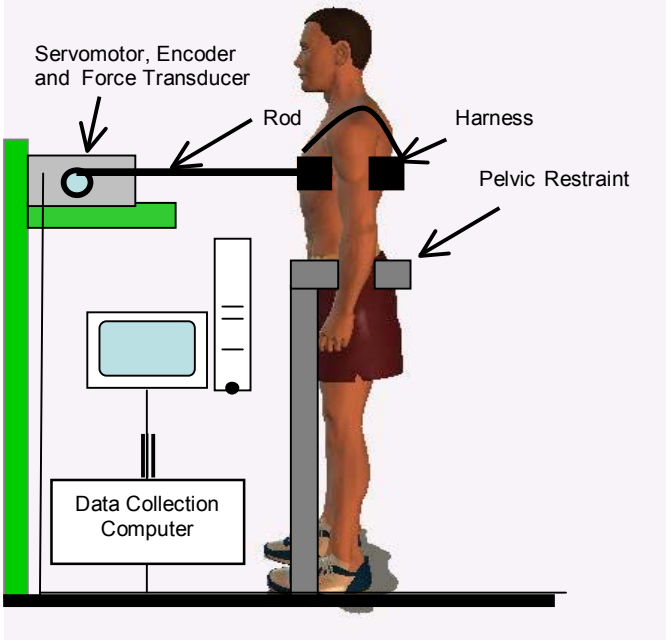

Figure 5.1 Experimental Setup. The servomotor applied a pseudorandom binary sequence (PRBS) of position perturbations to the T10 level of the trunk and the resulting force was measured. Subjects were securely strapped into a rigid structure to isolate movement to the trunk.

lateral and 2 cm. superior to the umbilicus; external obliques 10 cm. lateral to the umbilicus with the electrode pair at an angle of 45°; internal obliques 10 cm. lateral to the midline just superior to the iliac crest and inferior to the latissimus dorsi (lumbar triangle) at an angle of 45°; and erector spinae 4 cm. lateral to the L3 spinous process. A reference electrode was placed on a prominent bony section of the left tibia. The skin was cleansed with alcohol pads prior to attachment of the bipolar surface EMG electrodes. A signal check was performed to ensure quality of the EMG signals before each experimental session. All EMG data were band-pass filtered in hardware between 20 and 450 Hz and sampled at 1000 Hz. The EMG signals were rectified and filtered using a 75 Hz, low-pass, seventh-order Butterworth filter then normalized relative to the signal levels

collected during maximum voluntary contractions (MVC) in isometric flexion and extension tasks.

5.3.3 Experimental Protocol

Subjects were instructed to maintain isometric trunk extension exertion at pre-specified levels of 20% MVC, 35% MVC, and 50% MVC by observing a real-time video display of the applied force. They were instructed to relax their trunk flexor muscles during the extension exertions so as to minimize antagonistic co-contraction during the extension effort. In separate experimental conditions the subjects were instructed to maximally co-contract their abdominal muscles during a 20% MVC trunk extension exertion for comparison with minimal co-contraction conditions. Once steady-state exertion was achieved, a pseudo-random binary sequence (PRBS) of trunk perturbations was applied to the T10 level of the subject to cause small movement disturbances.

Movement sequences had a switching-rate of 150 ms. This means that the trunk was moved rapidly between two positions at random multiples of the switching-rate, i.e. pulse-width was 150 ms, 300 ms, 450 ms, 600 ms, or 750 ms (Figure 5.2). Two perturbation trials of 30 s each were performed at each exertion level and co-contraction condition for a total of 8 data trials per subject presented in random order. Kearney (1997) concluded that a peak-to-peak disturbance amplitude of 0.03 rad was ideal when studying the ankle joint because the sequences: (1) had an average velocity low enough to avoid attenuating reflex responses, (2) contained power over a wide enough bandwidth to

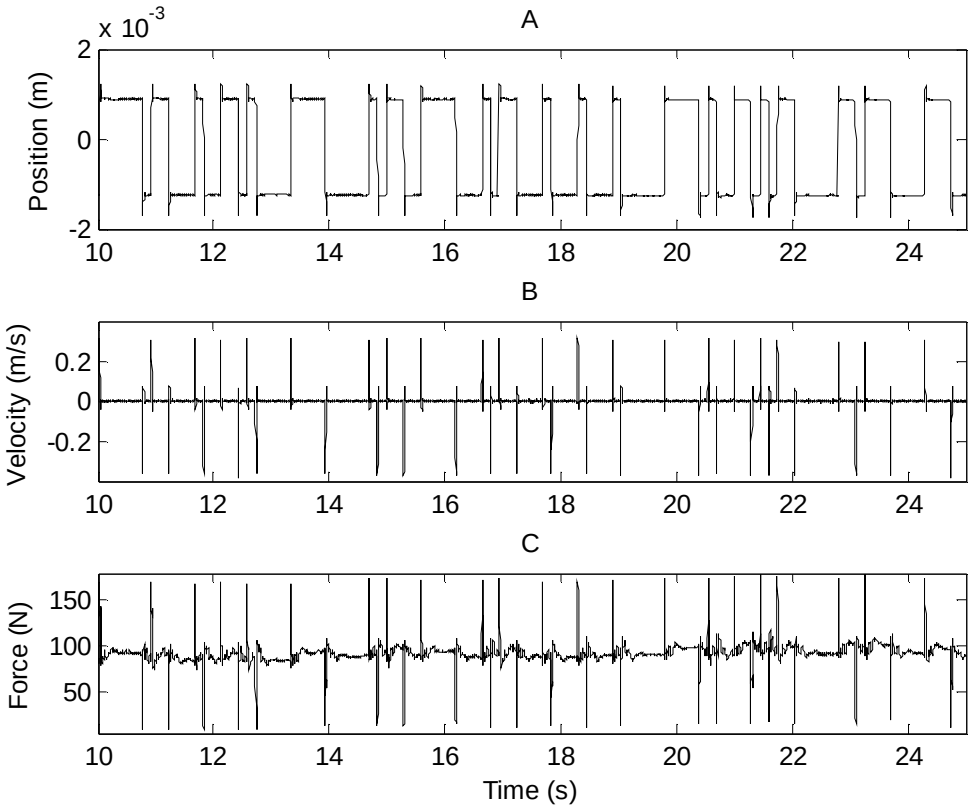

Figure 5.2A-B-C. Typical experimental record for a subject maintaining an extension exertion level of 35% MVC with minimal co-contraction.

identify the dynamics, and (3) permitted the subject to maintain a required tonic contraction throughout the perturbation sequence. It is unknown whether this level of perturbation amplitude is also ideal for the trunk, but our pilot studies indicated that position perturbations with a peak-to-peak amplitude of 2 mm (approximately 0.01 rad) were sufficient to meet the above criteria as well as exhibit a peak-to-peak rise time of 36.0 ± 1.6 ms, i.e. less than the reflex delay.

5.3.4 Analysis Procedures

Intrinsic and reflex dynamics were separated by nonlinear parallel-cascade system identification procedures. Briefly, the total measured force response associated with the position disturbance, F_{TOTAL}, is considered to be the sum of the forces attributed to intrinsic muscle stiffness, F_{INT}, and reflex force, F_{REF} (Figure 5.3).

$$F_{TOTAL} = F_{INT} + F_{REF} \tag{5.1}$$

In the intrinsic pathway H_{INT} describes the dynamic response to small position disturbances. These are attributed to the intrinsic stiffness of the active muscles with small contribution from the passive ligamentous structures of the torso and spine. The reflex pathway is modeled as a differentiator, in series with a delay, a static nonlinear element, $N_{REF}(.)$, and a dynamic linear element, H_{REF}. Both H_{INT} and H_{REF} are the transfer functions representing the dynamics contained within each pathway.

The nonlinear parallel-cascade system identification technique used to identify the dynamics of the intrinsic and reflex pathways proceeds as follows:

1) Intrinsic dynamics were estimated in terms of a linear impulse response function, H_{INT}, relating position and force. The length of this IRF was fixed at a value less than the reflex delay to ensure that forces due to reflex mechanisms would not influence the estimated, H_{INT}. Granata et al (2004) observed a reflex peak at 67 ms in the erector spinae muscles with response onset at approximately 50 ms. In order to provide an adequate cushion to guarantee all forces predicted by H_{INT} arose from intrinsic properties only with no reflex contamination, an IRF length of 40 ms was chosen for this analysis.

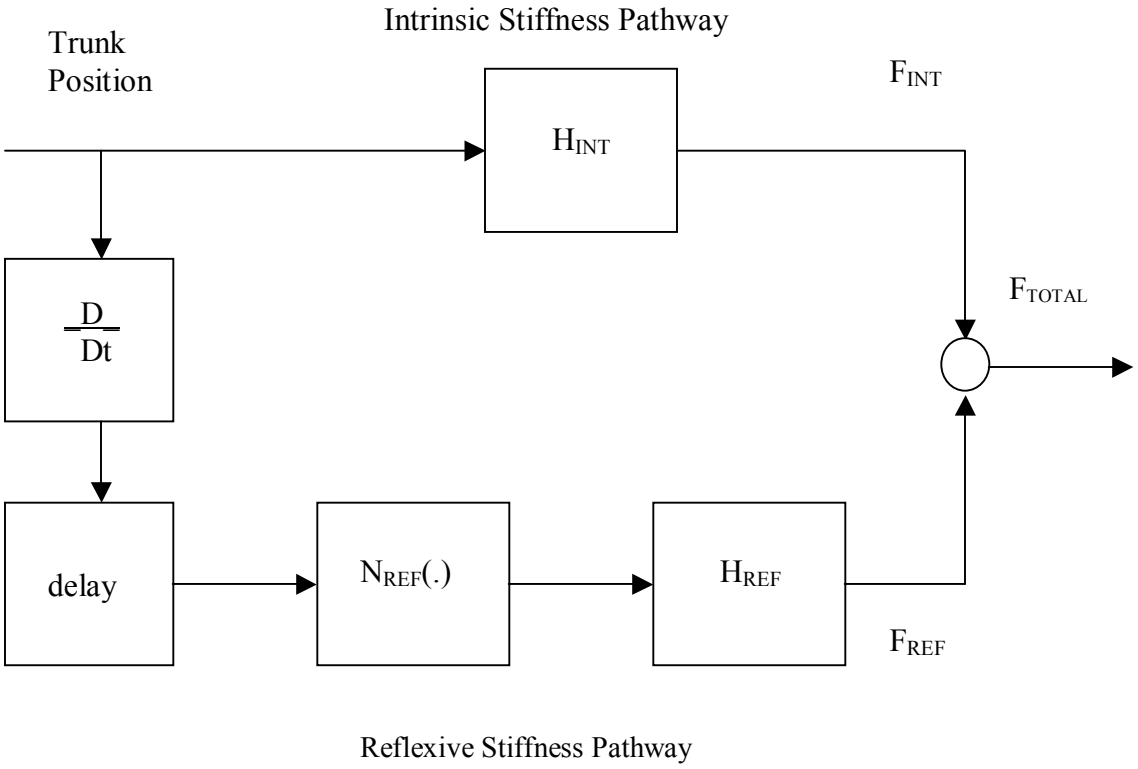

Figure 5.3. Block diagram showing the parallel cascade structure comprised of the intrinsic and reflexive contributions to overall trunk force.

2) H_{INT} was convolved with the input position to generate an estimate of the intrinsic force, $\overline{F}_{INT}$. By subtraction from the measured force, F_{TOTAL}, the component of force not attributable to intrinsic muscle dynamics was computed, $\overline{F}_{INT\,RESID}$. This residual force provided an initial estimate of the reflex force:

$$\overline{F}_{INT\,RESID} = F_{TOTAL} - \overline{F}_{INT} \tag{5.2}$$

3) The reflex pathway was investigated by treating velocity as the input and $\overline{F}_{INT\,RESID}$ as the output. A Hammerstein identification procedure (Hunter and Korenberg, 1986) was used to simultaneously identify both the static nonlinear, $N_{REF}(.)$, and linear

dynamic elements, H_{REF}. Interpretation of the static nonlinear element, $N_{REF}(.)$, revealed that it behaved as a half-wave rectifier, i.e. reflexes were elicited only during eccentric stretch of the paraspinal muscles.

4) This nonlinear model was used to generate a new estimate of the reflex force, $\overline{F}_{REF}$, by applying the static nonlinearity to the measured velocity signal and convolving H_{REF} with the transformed velocity. The reflex-residual force, $\overline{F}_{REF\ RESID}$ was computed by subtraction from the measured force, F_{TOTAL}. This residual force was attributed to the intrinsic force and the estimation procedure was repeated starting at the first step using the new $\overline{F}_{INT} \approx \overline{F}_{REF\ RESID}$ as the output signal in the estimation of H_{INT}.

$$\overline{F}_{REF\ RESID} = F_{TOTAL} - \overline{F}_{REF} \tag{5.3}$$

5) The net predicted force, $\overline{F}_{TOTAL}$ was formed from the sum of the estimated intrinsic and reflex components

$$\overline{F}_{TOTAL} = \overline{F}_{INT} + \overline{F}_{REF} \tag{5.4}$$

The percentage variance accounted for, VAF_{TOTAL}, was computed as the normalized error between the actual and estimated total force

$$VAF_{TOTAL} = 100\left(1 - \frac{\sum\left(F_{TOTAL} - \overline{F}_{TOTAL}\right)^2}{\sum\left(F_{TOTAL}\right)^2}\right) \tag{5.5}$$

The procedure was continued until successive iterations failed to improve VAF_{TOTAL}.

5.3.5 Parametric Model

Parametric estimates of intrinsic stiffness dynamics can be obtained by inverting the intrinsic impulse response function, H_{INT}, to obtain the compliance IRF, H_{COMP}. Compliance IRFs can then be parameterized by a least-squares fit to the second-order system shown in equation (5.6):

$$H_{COMP}(s) = \frac{1}{Ms^2 + Bs + P_{INT}} \tag{5.6}$$

where

$$P_{INT} = k_{INT} - Mgh \tag{5.7}$$

In equations (5.6) and (5.7), M is the effective trunk mass, B is the intrinsic muscle damping, k_{INT} is the intrinsic muscle stiffness, and s is the Laplace variable. P_{INT} is the proportional intrinsic response including the intrinsic muscle stiffness and the gravitational moment about the trunk where g is the acceleration due to gravity, and h is the height of the trunk center of mass. The proportional intrinsic response, P_{INT}, provides an assessment of stability because it represents the antagonistic effects of the "stabilizing" muscle stiffness and the "destabilizing" gravitational moment.

Similar parameterization to equation (5.6) has been successfully performed in studies that involve a largely positive value for the proportional intrinsic response, P_{INT}. Such studies include the investigation of intrinsic ankle dynamics (Kearney et al., 1997; Mirbagheri et al., 2000) where the gravitational moment is essentially negligible. In the present study, the large gravitational mass of the trunk resulted in values of P_{INT} that were negative or near zero. This indicates unstable dynamic behavior and results in an unbounded compliance function which can not be parameterized with a standard second-

order compliance model such as equation (5.6). In order to obtain a quantitative measure of the intrinsic stiffness of the system a static calculation of P_{INT} was performed by examining the final estimated intrinsic force signal, $\overline{F}_{INT}$, and determining the change in steady-state force which results from the 2 mm position perturbation as shown in equation (5.8):

$$P_{INT} = \frac{\Delta \overline{F}_{INT}, N}{0.002, m} \tag{5.8}$$

The reflexive stiffness impulse response function, H_{REF}, was parameterized by using a model comprising a standard second-order lowpass system in series with a delay:

$$H_{REF}(s) = \frac{G_{REF}}{s^2 + 2\zeta\omega_n s + \omega_n^2} e^{-sT} \tag{5.9}$$

where G_{REF} is the static reflex gain, ζ is the damping parameter, ω_n is the undamped natural frequency, T is the conduction delay associated with the reflex pathway, and s is the Laplace variable. Parameters were estimated by obtaining the best least-squares fit between H_{REF} and equation (5.9). Prior to parameterization, H_{REF} was visually inspected to determine the most suitable value for the reflex delay, and T = 40 ms was found to be most appropriate.

5.3.6 Statistical Analysis

Statistical repeated measures analyses (ANOVA) were performed to determine the effect of trunk extension exertion level and cocontraction on the proportional intrinsic response, P_{INT}, and the reflexive stiffness parameters (G_{REF}, ζ, ω_n). Analyses were

performed using commercial statistical software (Statistica 5, Statsoft, Inc., Tulsa, OK) using a significance level of $\alpha < 0.05$ for all tests. Trends in significant variables were investigated using Tukey honest significant difference (HSD) post hoc analyses.

5.4 Results

Figure 5.2 shows a typical experimental record obtained while a subject maintained an exertion level of 35% MVC with minimal co-contraction. Figure 5.2A shows the applied position perturbations, Figure 5.2B shows the numerically differentiated velocity of the applied position perturbations, and Figure 5.2C shows the corresponding trunk force.

Typical intrinsic force response, $\overline{F}_{INT}$, to a pseudorandom binary sequence of small position perturbations are illustrated for a subject demonstrating a small positive value of P_{INT} (Figure 5.4B) and a subject demonstrating a small negative value of P_{INT} (Figure 5.4C). Both subjects exhibit an immediate large inertial spike in the direction of the position perturbation, followed by a steady-state intrinsic force that tracks the perturbation sequence. The difference between these two subjects can be seen in the polarity difference in the steady-state intrinsic force. Shift of this steady-state force is positively correlated, i.e. in the same direction, with the position change for a positive value of P_{INT} (Figure 5.4B). It is negatively correlated, i.e. in the opposite direction, with the position change for a negative value of P_{INT} (Figure 5.4C).

The nonlinear parallel-cascade system identification procedure was able to accurately predict the total force response of the trunk to the pseudorandom position perturbations with an accuracy of $VAF_{TOTAL} = 80.9 \pm 3.6$ %. VAF_{TOTAL} was not significantly influenced by exertion level ($p = 0.74$) or co-contraction ($p = 0.51$). This suggests the analyses accurately represented the torso dynamics regardless of the experimental condition.

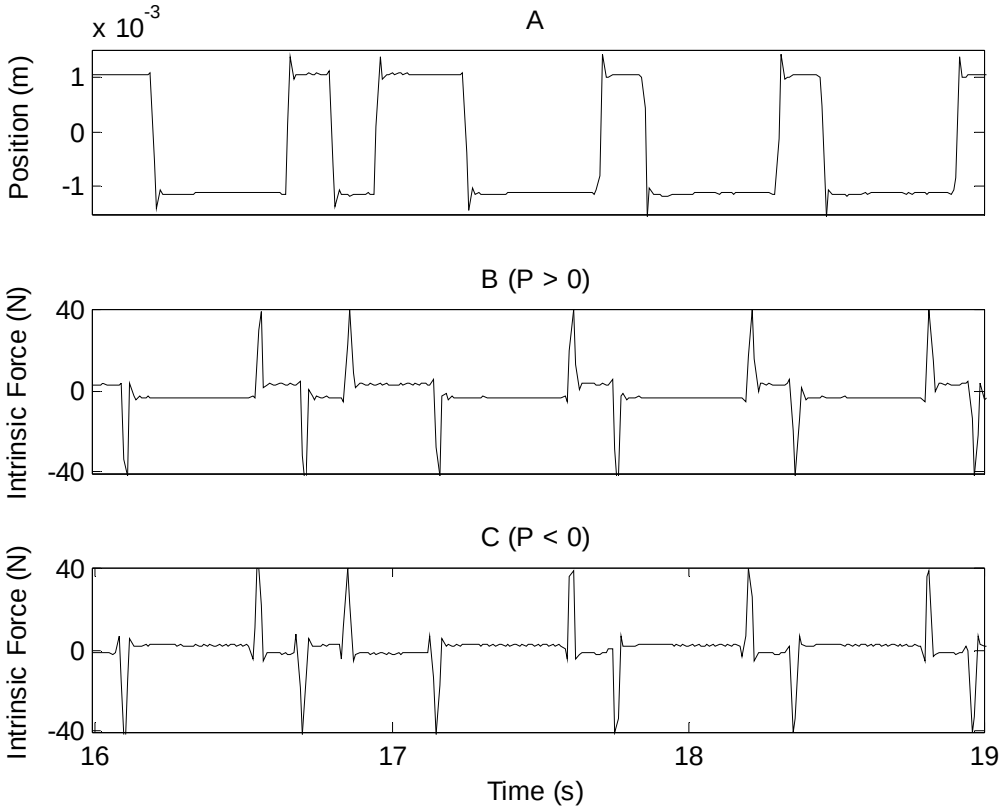

Figure 5.4A-B-C. Intrinsic force response to a pseudorandom binary sequence of small position perturbations for a subject demonstrating a small positive value of P_{INT} (B) and a subject demonstrating a small negative value of P_{INT} (C).

Mean value of the proportional intrinsic response, P_{INT}, was -0.0219 ± 0.350 N/mm. P_{INT} was found to increase significantly with extension exertion force ($p < .01$). P_{INT} increased from -0.415 N/mm at the lowest exertion level to +0.421 N/mm at the highest exertion level (Table 5.1). P_{INT} also exhibited a significant increase with co-contraction ($p < .05$), increasing from -0.415 to -0.136 N/mm.

The reflexive stiffness IRF, H_{REF}, was able to predict the reflexive force occurring as a result of the position perturbations with an accuracy of 74.1 ± 2.0 % and was not significantly influenced by exertion level ($p = 0.71$) or co-contraction ($p = 0.65$). The

Table 5.1. Mean values of the proportional intrinsic response (P_{INT}) and reflexive stiffness parameters (G_{REF}, ζ, w_n) for each experimental condition

	20% MVC	35 % MVC	50 % MVC	20% MVC co-contract	Mean
P_{INT} (N/mm)	-0.415 (0.044)	0.043 (0.027)	0.421 (0.099)	-0.136 (0.142)	**-0.022 (0.350)**
G_{REF} (N-s/m)	197 (32.0)	221 (34.8)	248 (42.5)	167 (27.5)	**208 (34.5)**
ζ	0.662 (0.020)	0.546 (0.064)	0.530 (0.010)	0.419 (0.007)	**0.539 (0.099)**
w_n (Hz)	8.69 (0.376)	9.54 (0.178)	9.16 (0.020)	9.13 (0.135)	**9.13 (0.344)**

parametric model fit the reflexive stiffness with an accuracy of 74.4 ± 2.8 % and was also not significantly influenced by exertion level ($p = 0.21$) or co-contraction ($p = 0.24$). A typical reflexive stiffness IRF is shown in Figure 5.5 along with the superimposed second-order least-squares fit.

Mean value of reflexive stiffness gain, G_{REF}, was 208 ± 34.5 N-s/m and increased significantly with exertion level ($p < .05$). It increased from 197 N-s/m at the lowest exertion level to 248 N-s/m at the highest exertion level (Table 5.1). Reflexive stiffness gain did not vary with co-contraction ($p = 0.27$).

The mean reflexive undamped natural frequency was 9.13 ± 0.344 Hz and also did not vary with exertion level ($p = 0.71$) or co-contraction ($p = 0.77$) (Table 5.1). The

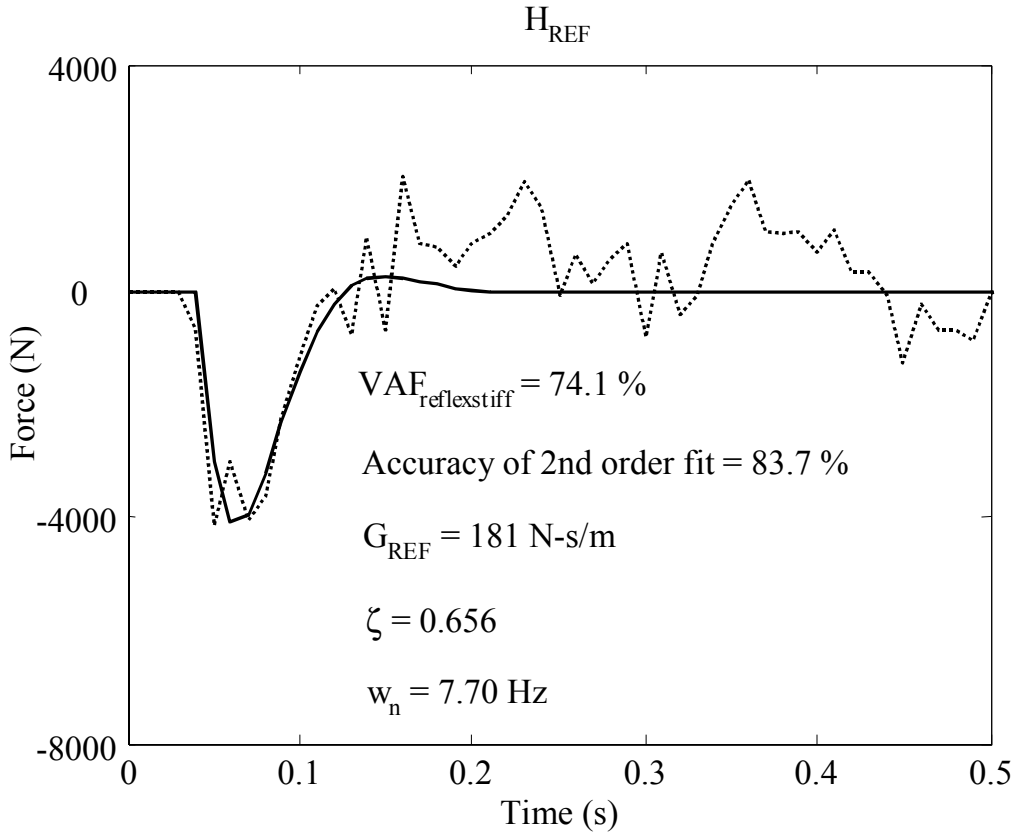

Figure 5.5. Reflexive stiffness impulse response function, H_{REF}, along with the superimposed second-order least-squares fit for a subject maintaining an extension exertion level of 20% MVC with minimal co-contraction.

mean reflexive damping parameter, ζ, was 0.539 ± 0.099 and did not vary with exertion level ($p = 0.09$) or co-contraction ($p = 0.08$) (Table 5.1). These data suggest the time behavior of the reflex response was not influenced by experimental conditions whereas the amplitude of the reflex response was significantly influenced by exertion force.

5.5 Discussion

The goal of this study was to determine the relative contributions of intrinsic muscle stiffness and reflexive response to spinal stability and trunk dynamics. The proportional intrinsic response, P_{INT}, was defined as position-dependant factors that contribute to overall trunk dynamics before the onset of the reflex response. P_{INT} includes the destabilizing effects of gravity and the restorative forces associated with passive tissue stiffness and intrinsic stiffness of active muscles. If the spine and torso are disturbed slightly from the equilibrium posture then intrinsic stiffness provides restorative forces that tend to return the posture toward the equilibrium state, i.e. positive contribution to P_{INT}. Intrinsic torso stiffness is attributed primarily to active muscle elasticity (Gardner-Morse et al., 1995; Panjabi, 1992b) with small contributions from passive tissues. Conversely, gravitational mass contributes destabilizing forces that tend to drive the posture away from the equilibrium state following a small disturbance, i.e. negative contribution to P_{INT}. To be considered stable the system must be drawn toward the equilibrium posture (Nayfeh and Balachandran, 1994) thereby requiring that the combined effects of P_{INT} and the reflex response must be positive.

Results revealed that the intrinsic stiffness alone was insufficient to stabilize gravitational effects of torso mass and external loads during active voluntary trunk extension exertions. This was apparent from the negative value of P_{INT}, i.e., the negative contribution of gravitational mass was often greater than the positive contribution of the intrinsic muscle stiffness and passive tissue stiffness. Reflex response contributed to the stabilizing dynamics of the torso. Without the reflex response the system was often

unstable, thereby indicating that the reflex contribution is a necessary component of the stabilizing neuromuscular behavior.

P_{INT} was sensitive to the voluntary trunk extension effort (Table 5.1) and increased significantly from -0.415 N/mm at the lowest exertion level to +0.421 N/mm at the highest exertion level ($p < .01$). This agrees with previously published trends, joint stiffness increases with the level of voluntary effort and muscle activity (Gardner-Morse and Stokes, 2001; Lee et al., 2005). At efforts of 20 % MVC, P_{INT} was negative indicating unstable dynamic behavior, thereby requiring the contribution of the reflex response to maintain spinal stability. These unstable dynamics became stable with increased effort illustrated by positive values of P_{INT}. However, in a lifting environment, it is possible that P_{INT} may not achieve positive stable behavior with increased extension exertion. The experiment was designed to resist trunk extension force with a servomotor and load cell. The destabilizing effects of the gravitational mass were therefore independent of the exertion effort. Hence, the increase in P_{INT} with exertion effort was a consequence of increased intrinsic muscle stiffness while the protocol prohibited destabilizing increase in gravitational effects. Conversely, if increased extension effort had been achieved by requiring subjects to hold weight of increasing mass in their hands, then the destabilizing gravitational mass effects would increase in proportion to the exertion effort. It is possible in that case that P_{INT} may not become positive, i.e. remain unstable, with increased effort in a lifting paradigm.

P_{INT} increased significantly with co-contraction, -0.415 to 0.136 N/mm. These effects were expected as it has been previously established that joint stiffness increases with co-contraction (Lee et al., 2005; Cholewicki et al., 1997). P_{INT} appears to increase

more with isolated extensor contraction than with maximal co-contraction even though co-contraction is considered one of the primary mechanisms for increasing the overall stiffness and stability of the spine. The difference between co-contraction conditions was equivalent to a 10 % MVC change in extension force. This effect may partly be a result of the subject's inability to perform the experimental task without abdominal muscle co-contraction. Analyses of the rectus abdominus (RA) EMG during the perturbation sequence revealed a mean activation level of 34.9 % MVC during the minimal co-contraction trials and 76.2 % MVC during the maximal co-contraction trials. Co-contraction may have been necessary to maintain the prescribed extensor force during the perturbation sequence.

Eight of the eleven subjects demonstrated a negative mean value of P_{INT}. Of these eight subjects three demonstrated negative values of P_{INT} under all experimental conditions, including the 50 % MVC and co-contraction trials. The other five exhibited a positive value of P_{INT} only at the 50 % MVC condition. Conversely, all three subjects who exhibited a positive mean value of P_{INT} demonstrated a positive value of P_{INT} under all conditions. These results suggest notable subject-to-subject differences in intrinsic neuromuscular stability. However, even in those subjects who demonstrated positive values of P_{INT}, the values were small. Whether the subject-to-subject differences in intrinsic stabilizing muscle behavior contributes to risk of low-back-pain should be investigated in future research.

The mean value of P_{INT} was -0.0219 ± 0.350 N/mm which was not significantly different than zero ($p = 0.74$). Since P_{INT} consists of the antagonistic effects of the positive intrinsic muscle stiffness, k_{INT}, and the negative gravitational moment about the

trunk, Mgh, the near zero mean value for P_{INT} indicates the two components have similar magnitudes. An estimate of the magnitude of the gravitational moment can be obtained by calculating the trunk mass, M, and the trunk center of mass, h, for each subject based on subject anthropometry (Winter, 1990). This gravitational moment can then be used in conjunction with equation (5.7) to estimate the intrinsic muscle stiffness, k_{INT}. The mean value for the gravitational moment was -1.70 ± 0.4 N/mm and the mean value of intrinsic muscle stiffness was k_{INT} = 1.68 ± 0.4 N/mm.

For the sake of comparison, we calculated the effective trunk stiffness, k_{EFF}, using an analysis procedure as in Moorhouse and Granata (2005). Mean effective trunk stiffness was 5.35 ± 0.85 N/mm. This represents the total trunk stiffness that includes the effects of both intrinsic and reflex dynamics. The difference between the effective stiffness and intrinsic stiffness values can be attributed to the reflex contribution to torso dynamics. Moorhouse and Granata (2005) applied a PRBS of force perturbations to the trunk and obtained an effective trunk stiffness value of 2.78 N/mm, i.e. about the half the value calculated in this study. The difference in effective stiffness between the two studies might be attributed to the difference in experimental protocol, i.e. position perturbations versus force perturbations, and the higher velocity perturbations applied in this study that may have elicited a larger reflex response.

In all subjects the reflex response contributed to the stabilizing control of the spine and torso. Recognizing that the mean effective trunk stiffness was the sum of the proportional intrinsic, P_{INT}, and reflex contributions, then we can estimate the mean reflex contribution as 5.37 ± 0.85 N/mm. Recall that the mean intrinsic stiffness value,

k_{INT}, was 1.68 ± 0.4 N/mm. Therefore, approximately 75 % of the trunk stiffness can be attributed to the reflex response.

Reflex gain, G_{REF}, represents a measure of the magnitude of restorative forces, analogous to the intrinsic stiffness, which are contributed by the reflex response. G_{REF} increased significantly with exertion, i.e. 197 N-s/m at 20 % MVC and 248 N-s/m at 50 % MVC. Research suggests that motor neurons that initiate reflexive action are influenced by muscle tone and that reflex excitation tends to increase with the pre-activation of muscle (Matthews, 1986; Bennett et al., 1994). This additional reflex excitation induces corresponding mechanical response until the saturation point of 50% MVC at which point additional neuronal excitation fails to have mechanical consequences. Since the highest voluntary contraction investigated in this study was 50% MVC the increase in reflexive stiffness gain with the level of extension exertion level was in agreement with previous studies. Hence, the reflex gain increases in proportion to the intrinsic stiffness with greater exertion effort thereby contributing to stabilizing control of the spine throughout a broad range of measured extension efforts.

This study revealed some interesting insight into the significant role that reflexes play in trunk dynamics and consequential spinal stability. Previous spinal stability models neglect the mechanical effects of reflex responses. Results of this study indicate that any comprehensive spinal stability model should include the role of reflexes, as they may account for 75 % of the stabilizing dynamics of the torso. This estimate of the role of reflexes is somewhat limited in that the gravitational moment was not actually measured, but calculated based on estimates of the subjects trunk mass, M, and their trunk center of mass, h, obtained from anthropometric tables (Winter, 1990). This

estimate of the gravitational moment was used to generate k_{INT} which was then used to determine the percent contribution of reflexes to the total stiffness. However, even a 10 % error in the estimation of the gravitational moment would result in only a 2 % error in the percentage contribution of reflexes.

The failure of intrinsic muscle stiffness alone to counteract the destabilizing effects of gravity may explain why many injuries occur due to sudden slips or unexpected loads that challenge the stability of the spine before reflexes are able to activate (Manning and Shannon, 1981). It also may reveal why many injuries occur during the lifting of light objects rather than heavy objects. The intrinsic stiffness of the spine was shown to increase with the level of muscle contraction so the lack of muscle contraction necessary to perform light load tasks results in more of the spinal stability responsibility to be shouldered by the neuromuscular control system, leaving the spine somewhat vulnerable to random neuromuscular errors or sudden kinematic perturbations. These results also indicate that individuals with disturbed reflex response may be more susceptible to spinal instability events. Future studies should further examine the effect of variables such as fatigue, gender, and initial trunk angle on the intrinsic stiffness and reflex dynamics of the trunk.

5.6 Acknowledgements

This research was supported in part by a grant R01 AR46111 from CDC / National Institute for Occupational Safety and Health. We wish to thank T. Franklin and S. Hanson for their assistance in data collection.

Conclusions

Spinal stability describes the ability of the neuromuscular system to maintain equilibrium in the presence of kinematic and control variability, and may play an important role in the etiology of low-back disorders (LBDs). If the spine is insufficiently stable during loading there is increased risk that natural kinematic variability (i.e., small kinematic perturbations) or recruitment variability (i.e., small neuromuscular errors) will be amplified by biomechanical forces to cause sudden undesired vertebral motion (localized spinal column buckling) and strain damage of intervertebral tissues. This damage to the intervertebral tissues can result in intervertebral hypermobility and potential neuromotor abnormalities. Furthermore, this damage may induce pain, further reduce spinal stability, and enhance the risk of injury or re-injury.

The primary mechanism for the neuromuscular control of spinal stability is the recruitment and control of active paraspinal muscle stiffness (i.e., trunk stiffness). The two major components of active muscle stiffness include the immediate stiffness contribution provided by the intrinsic stiffness of actively contracted muscles, and the delayed stiffness contribution provided by the reflex response. The combined behavior of these two components of active muscle stiffness is often referred to as "effective stiffness".

The goal of this study was to quantify the effective dynamics of the trunk as well as separate these dynamics into their intrinsic and reflexive components in an effort to understand the neuromuscular control of spinal stability. Stochastic system identification techniques were utilized and nonparametric impulse response functions (IRFs) calculated in three separate studies in an effort to:

1) **Quantify the effective dynamics (stiffness, damping, mass) of the trunk**

Nonparametric IRFs were implemented to estimate the dynamics of the trunk during active voluntary trunk extension exertions. IRFs were determined from the movement following pseudo-random stochastic force disturbances applied to the trunk. The nonparametric IRFs successfully accounted for 88% of the trunk movement variance. A second-order model of trunk dynamics was fit to the IRF with 96% accuracy. Results demonstrated a significant increase in effective stiffness and damping with voluntary exertion forces.

2) **Quantify the reflex dynamics of the trunk**

Nonparametric IRFs were computed to quantify both the reflex delay and reflex gain of the paraspinal muscles. Using a similar pseudo-random force disturbance protocol, the muscle electromyographic (EMG) reflex response was successfully characterized with a variance accounted for (VAF) of 48%. Reflexes were observed in 81% of the trials at a mean response delay of 67 msec. Reflex gain was estimated from the peak of the IRF and increased significantly with exertion effort.

3) **Separate the intrinsic and reflexive components of the effective dynamics and determine the relative role of each in the control of spinal stability.**

Both intrinsic muscle and reflex components of activation contribute to the effective trunk stiffness. To evaluate the relative role of these components, a nonlinear parallel-cascade system identification procedure was used to separate the intrinsic and reflexive dynamics. Results revealed that the intrinsic dynamics of the trunk alone can be

insufficient to counteract the destabilizing effects of gravity. This illustrates the extreme importance of reflexive feedback in the maintenance of spinal stability and warrants the inclusion of reflexes in any comprehensive trunk model.

This study revealed some interesting insight into the significant role that reflexes play in trunk dynamics and consequential spinal stability. Previous spinal stability models neglect the mechanical effects of reflex responses. Results of this study indicate that any comprehensive spinal stability model should include the role of reflexes, as they may account for 75 % of the stabilizing dynamics of the torso.

The failure of intrinsic muscle stiffness alone to counteract the destabilizing effects of gravity may explain why many injuries occur due to sudden slips or unexpected loads that challenge the stability of the spine before reflexes are able to activate (Manning and Shannon, 1981). It also may reveal why many injuries occur during the lifting of light objects rather than heavy objects. The intrinsic stiffness of the spine was shown to increase with the level of muscle contraction so the lack of muscle contraction necessary to perform light load tasks results in more of the spinal stability responsibility to be shouldered by the neuromuscular control system, leaving the spine somewhat vulnerable to random neuromuscular errors or sudden kinematic perturbations. These results also indicate that individuals with disturbed reflex response may be more susceptible to spinal instability events. Future studies should further examine the effect of variables such as fatigue, gender, and initial trunk angle on the intrinsic stiffness and reflex dynamics of the trunk.

References

Agarwal, G.C., Gottlieb, C.L., 1977. Compliance of the human ankle joint. Transactions of the American Society for Mechanical Engineers 99, 166-170.

Andersson, G.B.J., 1981. Epidemiologic aspects on low back pain in industry. Spine 6, 53-60.

Avela, J., Kyrolainen, H., & Komi, P. V. 1999, Altered reflex sensitivity after repeated and prolonged passive muscle stretching, J.Appl.Physiol., 86, 1283-1291.

Bendat, J.S., Piersol, A.G., 2000. Random data: analysis and measurement procedures, 3 edn. New York: John Wiley & Sons.

Bennett, D. J., Gorassini, M., & Prochazka, A. 1994, Catching a ball: contributions of intrinsic muscle stiffness, reflexes, and higher order responses, Can.J Physiol Pharmacol., 72, 525-534.

Bergmark, A., 1989. Stability of the lumbar spine: A study in mechanical engineering. Acta Orthopaedica Scandinavica Supplementum 60, 1-54.

Berne, R.M., Levy, M.N., 1998. Physiology. 4th edition. St. Louis, MO: Mosby, Inc.

Bull Andersen, T., Essendrop, M., Schibye, B., 2004. Movement of the upper body and muscle activity patterns following a rapidly applied load: the influence of pre-load alterations. European Journal of Applied Physiology 91, 488-492.

Carter, R.R., Crago, P.E., Keith, M.W., 1990. Stiffness regulation by reflex action in the normal human hand. Journal of Neurophysiology 64, 105-118.

Cats-Baril, W., Frymoyer, J.W., 1991. The economics of spinal disorders. Edited by Frymoyer, J.W.; Ducker, T.B.; Hadler, N.M.; Kostuik, J.P.; Weinstein, J.N.; and Whitecloud, T.S. The Adult Spine (New York: Raven Press), pp. 85-105.

Cholewicki, J., McGill, S.M., 1996. Mechanical stability of the in vivo lumbar spine: Implications for injury and chronic low back pain. Clinical Biomechanics 11, 1-15.

Cholewicki, J., Panjabi, M.M., and Khachatryan, A., 1997. Stabilizing function of trunk flexor-extensor muscles around a neutral spine posture. Spine 22, 2207-2212.

Cholewicki, J., Juluru, K., Radebold, A., Panjabi, M.M., and McGill, S.M., 1999. Lumbar spine stability can be augmented with an abdominal belt and/or increased intra-abdominal pressure. European Spine Journal 8, 388-395.

Cholewicki J., Simons A.P.D., Radebold, A., 2000. Effects of external trunk loads on lumbar spine stability. Journal of Biomechanics 33, 1377-1385.

Claude, L. N., Solomonow, M., Zhou, B. H., Baratta, E. R. V., & Ping, M. 2003, Neuromuscular dysfunction elicited by cyclic lumbar flexion, Muscle & Nerve, 27, 348-358.

Crisco, J.J., Panjabi, M.M., 1992. Euler stability of the human ligamentous lumber spine: part I theory. Clinical Biomechanics 7, 19-26.

Dickey, J. P., McNorton, S., & Potvin, J. R. 2003, Repeated spinal flexion modulates the flexion–relaxation phenomenon, Clin.Biomech., 18, 783-789.

Dolan P., Earley M., & Adams M.A. 1994, Bending and compressive stresses acting on the lumbar spine during lifting activities, J.Biomechanics, 27, 1237-1248.

Enoka, R.M., 1994. Neuromechanical Basis of Kinesiology. 2nd ed. Champaign, IL: Human Kinetics

Gardner-Morse, M., Stokes, I.A.F., and Laible, J.P., 1995. Role of muscles in lumbar stability in maximum extension efforts. Journal of Orthopaedic Research 13, 802-808.

Gardner-Morse, M. G. & Stokes, I. A. F. 1998, The effects of abdominal muscle coactivation on lumbar spine stability, Spine, 23, 86-92.

Gardner-Morse, M., Stokes, I.A., 2001. Trunk stiffness increases with steady state effort. Journal of Biomechanics 34, 457-463.

Gedalia, U., Solomonow, M., Zhou, B. H., Baratta, R. V., Lu, Y., & Harris, M. 1999, Biomechanics of increased exposure to lumbar injury caused by cyclic loading - Part 2. Recovery of reflexive muscular stability with rest, Spine, 24, 2461-2467.

Godfrey, K.R., Correlation Methods. Automatica, 16527-16534.

Granata, K. P. & Marras, W. S. 1995, An EMG assisted model of biomechanical trunk loading during free-dynamic lifting, J.Biomechanics, 28, 1309-1317.

Granata, K. P., Orishimo, K., & Sanford, A. H. 2001, Trunk Muscle Coactivation in Preparation for Sudden Load, J.Electromyo.Kinesiol., 11, 247-254.

Granata, K.P., Orishimo, K., Sanford, A.H., 2002. Trunk muscle coactivation in preparation for sudden load. Journal of Electromyography and Kinesiology 11, 247-254.

Granata K.P., Wilson S.A., and Padua D.A, 2002. Gender differences in active musculoskeletal stiffness. Part I. Quantification in controlled measurement of knee joint dynamics. Journal of Electromyography and Kinesiology 12, 119-126.

Granata, K.P., Slota, G.P., Bennett, B.C., 2004. Paraspinal muscle reflex dynamics. Journal of Biomechanics 37, 241-247.

Granata, K.P., Rogers, E., Moorhouse, K.M., 2005. Effects of Static-relaxation on paraspinal reflex behavior. Clinical Biomechanics 20 (2005) 16-24

Herman, R., Freedman, W., Mayer, N., 1974. Neurophysiologic mechanisms of hemiplegic and paraplegic spasticity: implication for therapy. Archives of Physical and Medical Rehabilitation, 55, 338-343.

Hodges, P.W. and Richardson, C.A., 1996. Inefficient muscular stabilization of the lumbar spine associated with low back pain. A motor control evaluation of transversus abdominis. Spine 21, 2640-2650.

Hoffer, J.A., Andreassen, S., 1981. Regulation of soleus muscle stiffness in premammillary cats: intrinsic and reflex components. Journal of Neurophysiology 45, 267-285.

Hollbrook, T.L., Grazier, K., Kelsey, J.L., and Stauffer, R.N., 1994. The frequency of occurrence, impact and cost of selected musculoskeletal conditions in the United States.

Holm, S. H., Indahl, A., & Solomonow, M. 2002, Sensorimotor control of the spine, J.Electromyogr.Kinesiol., 12, 219-234.

Houk, J.C., Singer, J.J., Goldman, M.R., 1970. An evaluation of length and force feedback to soleus muscles of decerebrate cats. Journal of Neurophysiology 33, 784-811.

Hufschmidt, A., Mauritz, K.H., 1985. Chronic transformation of muscle in spasticity: a peripheral contribution to increased tone. Journal of Neurology, Neurosurgery, and Psychiatry 48, 676-685.

Hunter, I.W., Kearney, R.E., 1982. Dynamics of human ankle stiffness: variation with mean ankle torque. Journal of Biomechanics 15, 747-752.

Hunter, I.W., Kearney, R.E., 1983. Two-sided linear filter identification. Medical & Biological Engineering & Computing 21, 203-209.

Hunter, I.W., Korenberg, M.J., 1986. The identification of nonlinear biological systems: Wiener and Hammerstein cascade models. Biological Cybernetics 55, 135-144.

Jackson, M., Solomonow, M., Zhou B., Baratta, R. V., & Harras, M. 2001, Multifidus EMG and tension-relaxation recovery after prolonged static lumbar flexion, Spine, 26, 715-723.

Kang, Y.M., Choi, W.S., Pickar, J.G., 2002. Electrophysiologic evidence for an intersegmental reflex pathway between lumbar paraspinal tissues. Spine 27, E56-E63.

Kearney, R.E., Hunter, I.W., 1982. Dynamics of human ankle stiffness: variation with displacement amplitude. Journal of Biomechanics 15, 753-756.

Kearney, R.E., Hunter, I.W., 1983. System identification of human triceps surae stretch reflex dynamics. Experimental Brain Research 51, 117-127.

Kearney, R.E., Hunter, I.W., 1984. System identification of human stretch reflex dynamics: tibialis anterior. Experimental Brain Research 56, 40-49.

Kearney, R.E., Hunter, I.W., 1988. Nonlinear identification of stretch reflex dynamics. Annals of Biomedical Engineering 16, 79-94.

Kearney, R.E., Hunter, I.W., 1990. System identification of human joint dynamics. Critical Review of Biomedical Engineering 18, 55-87.

Kearney, R.E., Stein, R.B., Parameswaran, L., 1997. Identification of intrinsic and reflex contributions to human ankle stiffness dynamics. IEEE Transactions in Biomedical Engineering 44, 493-504.

Kelsey J.L., Githens, P.B., White A.A.III, and et al., 1984. An epidemiologic study of lifting and twisting on the job and risk for acute prolapsed lumbar intervertebral disc. Journal of Orthopedic Research 2, 61-66.

Kelsey, J.L., White, A.A., 1990. Epidemiology and impact of low back pain. Spine 5, 133-142.

Kerr, M., Frank, J., Harry, S., Norman, R. W., Wells, R., Neumann, P., & Claire, B. 2001, Biomechanical and psychophysical risk factors for low-back pain at work, Am J.Pub.Health, 91, 1069-1075.

Kippers, V. & Parker, A. W. 1984, Posture related to myoelectric silence of erectors spinae during trunk flexion, Spine, 9, 740-745.

Krajcarski, S.R., Potvin, J.R., Chiang, J., 1999. The in vivo dynamic response of the spine to perturbations causing rapid flexion: effects of pre-load and step input magnitude. Clinical Biomechanics 14, 54-62.

Lavender, S.A., Mirka, G.A., Schoenmarklin, R.W., Sommerich, C.M., Sudhakar, L.R., Marras, W.S., 1989. The effects of preview and task symmetry on trunk muscle response to sudden loading. Human Factors 31, 101-115.

Lee, P.J., Rogers, E., Granata, K.P., 2005. Active trunk stiffness increases with co-contraction. Journal of Electromyography & Kinesiology (In Press).

Ljung, L. & Ljung, E. J. 1998, *System Identification: Theory for the User*, 2 edn, Prentice Hall, Upper Saddle River, NJ.

Ljung L, 1999. System identification: theory for the user, 2 edn. Upper Saddle River, NJ: Prentice Hall.

Luoto, S., Taimela, S., Hurri, A., Aalto, H., Pyykko, I., Alaranta, H., 1996. Psychomotor speed and postural control in chronic low back pain patients. A controlled follow-up study. Spine 21, 2621-2627.

Magnusson, M. L., Aleksiev, A., Wilder, D. G., Pope, M. H., Spratt, K., Lee, S. H., Goel, V. K., & Weinstein, J. N. 1996, Unexpected load and asymmetric posture as etiologic factors in low back pain., Eur.Spine J., 5, 23-35.

Manning, D.P., Shannon, H.S., 1981. Slipping accidents causing low-back pain in a gearbox factory. Spine 6, 70-72.

Marras, W.S., Rangarajulu, S.L., Lavender, S.A., 1987. Trunk loading and expectation. Ergonomics 30, 551-562.

Marras, W.S., Mirka, G.A., 1992. A comprehensive evaluation of trunk response to asymmetric trunk motion. Spine 17, 318-326.

Marras, W. S., Lavender, S. A., Leurgans, S. E., & et.al. 1993, The role of dynamic three-dimensional trunk motion in occupationally-related low back disorders: The effects of workplace factors, trunk position and trunk motion characteristics on risk of injury, Spine, 18, 617-628.

Matthews, P.B.C., 1972. Mammalian Muscle Receptors and Their Central Actions. London, Arnold.

Matthews, P. B. C. 1986, Observations on the automatic compensation of reflex gain on varying the pre-existing level of motor discharge in man, J.Physiol., 374, 73-90.

Matthews, P.B., 1991. The human stretch reflex and the motor cortex. Trends in Neurosciences 14, 87-91.

McGill, S. M. & Brown, S. 1992, Creep response of the lumbar spine to prolonged full flexion, Clin Biomech., 7, 43-46.

McGill, S., Seguin, J., Bennett, G., 1994. Passive stiffness of the lumbar torso in flexion, extension, lateral bending, and axial rotation. Effect of belt wearing and breath holding. Spine 19, 696-704.

Mcgill, S.M., Cholewicki, J., 2001. Biomechanical Basis for Stability: An Explanation to Enhance Clinical Utility. Journal of Orthopaedic & Sports Physical Therapy 31, 96-100.

McMahon, T.A., 1984. Muscles, Reflexes, and Locomotion. Princeton, N.J.: Princeton University Press.

Mirbagheri, M.M., Barbeau, H., Kearney, R.E., 2000. Intrinsic and reflex contributions to human ankle stiffness: variation with activation level and position. Experimental Brain Research 135, 423-436.

Moorhouse, K. M. & Granata, K. P., 2005. Trunk stiffness and dynamics during active extension exertions. Journal of Biomechanics 38, 2000-2007

Morgan, D.L., 1977. Separation of active and passive components of short-range stiffness of muscle. American Journal of Physiology 232, c45-c49.

Nachemson, A., 1966. The load on lumbar disks in different positions on the body. Clinical Orthopaedics and Related Research 45, 107-122.

Nayfeh, A.H., Balachandran, B., 1994. Applied Nonlinear Dynamics: Analytical, Computational, and Experimental Methods. New York: Wiley, John & Sons, Incorporated. ISBN: 0471593486.

Nichols, T.R. Houk, J.C., 1976. Improvement of linearity and regulation of stiffness that results from the actions of the stretch reflex. Journal of Neurophysiology 39, 119-142.

NIOSH, 1981. A Work Practices Guide for Manual Lifting. 81-122.

Noth, J., Matthew, H.R., Friedemann, H.H., 1984. Long latency reflex force of human finger muscles in response to imposed sinusoidal movements. Experimental Brain Research 55, 317-324.

Ogata, K., 1997. Modern Control Engineering, 3rd ed. Upper Saddle River, NJ: Prentice Hall.

Omino, K. & Hayashi, Y. 1992, Preparation of dynamic posture and occurrence of low back pain, Ergonomics, 35, 693-707.

Oppenheim, A.V., Willsky, A.S., 1997. Signals & Systems. 2 ed. Upper Saddle River, NJ: Prentice-Hall, Inc.

Panjabi, M.M., 1992a. The Stabilizing System of the Spine. Part I. Function, Dysfunction, Adaptation, and Enhancement. Journal of Spinal Disorders 5, 383-389.

Panjabi, M.M., 1992b. The stabilizing system of the spine. Part II. Neutral Zone and instability hypothesis. Journal of Spinal Disorders 5, 390-397

Parnianpour, M., Campello, M., & Sheikhzadeh, A. 1991, The effect of posture on triaxial trunk strength in different directions: Its biomechanical consideration with respect to incidence of low-back problems in construction industry, Intl.J.Ind.Ergon., 8, 279-287.

Pope, M.H., 1996. Occupational Risk Factors, St. Louis, Mo.

Pope, M.H., Aleksiev, A., Panagiotacopulos, N.D., Lee, J.S., Wilder, D.G., Friesen, K., Stielau, W., Goal, V.K., 2000. Evaluation of low back muscle surface emg signals using wavelets. Clinical Biomechanics 15, 567-573.

Praemer, A., Furner, S., and Rice, D.P., 1992. Musculoskeletal conditions in the United States.

Press, B.P., Flannery, S.A., Teukolsky, S.A., Vetterling, W.T., 1985. Numerical Recipes: The Art of Scientific Computing. Cambridge, U.K.: Cambridge Univ. Press, pp 523-528.

Punnet, L., Fine L.J., Keyserling, W.M., Herrin G.D., and Chaffin, D.B., 1991. Back disorders and non-neutral trunk postures of automobile assembly workers. Scandinavian Journal of Work and Environmental Health 17, 337-346.

Rack, P.M.H., Westbury, D.R., 1973. The short-range stiffness of active mammalian muscle. Journal of Physiology 229, 16-17

Radebold, A., Cholewicki, J., Polzhofer, G.A., Green, T.P., 2001. Impaired postural control of the lumbar spine is associated with delayed muscle response times in patients with chronic idiopathic low back pain. Spine 26, 724-730.

Rosenbaum, D. & Hennig, E. M. 1995, The influence of stretching and warm-up exercises on Achilles tendon reflex activity, J.Sports Sci., 13, 481-490.

Rowe, M.L., 1971. Low back disability in industry: An updated position. Journal of Occupational Medicine 13, 476-478.

Scholten, P.J.M., Veldhuizen, A.G., 1986. The bending stiffness of the trunk. Spine 11, 463-467.

Shultz, S. J., Carcia, C. R., & Perrin, D. H. 2004, Knee joint laxity affects muscle activation patterns in the healthy knee, J Electromyogr.Kinesiol., 14, 475-483.

Simon, S.R., 1994. Orthopaedic Basic Science. American Academy of Orthopaedic Surgery, Rosemont, IL.

Sinkjaer, T., Toft, E., Andreassen, S., Hornemann, B.C., 1988. Muscle stiffness in human ankle dorsiflexors: intrinsic and reflex components. Journal of Neurophysiology 60, 1110-1121.

Solomonow, M., Zhou, B.H., Harras M., Lu Y., and Baratta, R.V., 1998. The ligamento-muscular stabilizing system of the spine. Spine 23, 2552-2565.

Solomonow, M., Zhou, B.H., Baratta, R.V., Lu, Y., Harris, M., 1999. Biomechanics of increased exposure to lumbar injury caused by cyclic loading: part 1. Loss of reflexive muscular stabilization. Spine 24, 2426-2434.

Solomonow, M., Eversull, E., He, Z. B., Baratta, R. V., & Zhu, M. P. 2001, Neuromuscular neutral zones associated with viscoelastic hysteresis during cyclic lumbar flexion, Spine, 26, E314-E324.

Solomonow, M., Baratta, R. V., Banks, A., Freudenberger, C., & Zhou, B. H. 2003a, Flexion-relaxation response to static lumbar flexion in males and females, Clin.Biomech.(Bristol., Avon.), 18, 273-279.

Solomonow, M., Baratta, R. V., Zhou, B. H., Burger, E., Zieske, A., & Gedalia, A. 2003b, Muscular dysfunction elicited by creep of lumbar viscoelastic tissue, J Electromyogr.Kinesiol., 13, 381-396.

Solomonow, M., Zhou, B. H., Baratta, R. V., & Burger, E. 2003c, Biomechanics and electromyography of a cumulative lumbar disorder: response to static flexion, Clin.Biomech., 18, 890-898.

Stefani, R.T., Shahian B., Savant, C.J., Hostetter, G.H., 2002. Design of Feedback Control Systems, 4 edn. New York: Oxford University Press.

Stokes, I.A., Gardner-Morse, M., Henry, S.M., Badger, G.J., 2000. Decrease in trunk muscular response to perturbation with preactivation of lumbar spinal musculature. Spine 25, 1957-1964.

Thomas, J.S., Lavender, S.A., Corcos, D.M., Andersson, G.B.J., 1998. Trunk kinematics and trunk muscle activity during a rapidly applied load. Journal of Electromyography and Kinesiology 8, 215-225.

Thompson, J. M. T. and G. W. Hunt, 1984. The General Conservative Theory. Elastic Instability Phenomena. New York, John Wiley & Sons: 1-26

Twomey, L. T. & Taylor, J. R. 1982, Flexion creep deformation and hysteresis in the lumbar vertebral column, Spine, 7, 116-122.

Van Dieen, J. H., Cholewicki, J., & Radebold, A. 2003, Trunk muscle recruitment patterns in patients with low back pain enhance the stability of the lumbar spine, Spine, 28, 834-841.

Wilder, D.G., Aleksiev, A.R., Magnusson, M.L., Pope, M.H., Spratt, K.F., Goel, V.K., 1996. Muscular response to sudden load. A tool to evaluate fatigue and rehabilitation. Spine 21, 2628-2639.

Winter, D. A., 1990. Biomechanics and Motor Control of Human Movement. New York, Wiley-Interscience Publication

Zhang, L.Q., Rymer, W.Z., 1997. Simultaneous and nonlinear identification of mechanical and reflex properties of human elbow joint muscles. IEEE Transactions on Biomedical Engineering 44, 1192-1209.

Zhang, L.Q., Huang, H., Sliwa, J.A., Rymer, W.Z., 1999. System Identification of Tendon Reflex Dynamics. IEEE Transactions on Rehabilitation Engineering 7, 193-203.